

# On the origin of the narrow peak and the isospin symmetry breaking of the $X(3872)$

Sachiko Takeuchi<sup>1,4</sup>, Kiyotaka Shimizu<sup>2</sup>, and Makoto Takizawa<sup>3,4</sup>

<sup>1</sup>*Japan College of Social Work, Kiyose, Tokyo 204-8555, Japan*

<sup>2</sup>*Department of Physics, Sophia University, Chiyoda-ku, Tokyo 102-8554, Japan*

<sup>3</sup>*Showa Pharmaceutical University, Machida, Tokyo 194-8543, Japan*

<sup>4</sup>*Theoretical Research Division, Nishina Center, RIKEN, Saitama 351-0198, Japan*

\*E-mail: s.takeuchi@jcsu.ac.jp

8/6/2019

.....  
The  $X(3872)$  formation from the  $B$ -decay and its decay into the two-meson state are investigated by employing a coupled-channel two-meson model with the  $c\bar{c}$  state. This two-meson state consists of the  $D^0\bar{D}^{*0}$ ,  $D^+D^{*-}$ ,  $J/\psi\rho$ , and  $J/\psi\omega$  channels. The energy-dependent decay widths of the  $\rho$  and  $\omega$  mesons are taken into account. The interaction between  $D$  and  $\bar{D}^*$  mesons are taken to be consistent with a lack of the  $B\bar{B}^*$  bound state. The  $c\bar{c}-D\bar{D}^*$  coupling is taken as a parameter to fit the  $X(3872)$  peak energy. The coupling between the  $D\bar{D}^*$  and  $J/\psi\rho$  or the  $D\bar{D}^*$  and  $J/\psi\omega$  channels is determined with the help of a quark model.

It is found that the  $J/\psi\rho$  and  $J/\psi\omega$  peaks appear around the  $D^0\bar{D}^{*0}$  threshold under the reasonable assumptions and that their peaks are very narrow when they appear. It is also found that the large decay width of the  $\rho$  meson enhances the isospin  $I=1$  component in the decay spectra in the  $X(3872)$  energy region. The size of the  $J/\psi\pi^3$  peak we calculated is 1.29-2.38 times as large as that of the  $J/\psi\pi^2$ . The isospin symmetry breaking in the present model comes from the difference in the charged and neutral  $D$  and  $D^*$  meson masses, which seems to give a sufficiently large isospin mixing to explain the experiments. Also, the results suggest that one can judge whether the  $X(3872)$  is a bound state by looking into the ratio of the partial decay width of  $X(3872)$  in the  $D^0\bar{D}^{*0}$  channel to that in the  $J/\psi\rho$  channel. Moreover, the relative importance of the  $c\bar{c}-D\bar{D}^*$  coupling in the  $X(3872)$  can be evaluated from the ratio of the transfer strength of the  $D^+D^{*-}$  to that of the  $D^0\bar{D}^{*0}$  as well as from the ratio of the  $J/\psi\pi^3$  peak size to that of the  $J/\psi\pi^2$ .

## 1. Introduction

The  $X(3872)$  peak has been found first by Belle [1] in the  $J/\psi\pi\pi K$  observation from the  $B$  decay. Its existence was confirmed by various experiments [2–5]. The mass of  $X(3872)$  is found to be  $3871.68 \pm 0.17$  MeV, which is very close to or even corresponds to the  $D^0\bar{D}^{*0}$  threshold,  $3871.85 \pm 0.20$  MeV, within the experimental errors [6]. Whether it is a resonance or a bound state has not been determined by the experiments yet. The  $X(3872)$  full width is less than 1.2 MeV [7], which is very narrow for such a highly excited resonance. The CDF group performed the helicity amplitude analysis of the  $X(3872) \rightarrow J/\psi\pi^+\pi^-$  decay and

---

concluded that the state is  $J^{PC}=1^{++}$  or  $2^{-+}$  [8]. Recently, LHCb experiments determined that its quantum numbers are  $J^{PC} = 1^{++}$ , ruling out the possibility of  $2^{-+}$  [9].

The  $X(3872)$  is observed first in the  $J/\psi\pi^n$  spectrum from the  $B$  decay. Later, the peak in the final  $D^0\bar{D}^{*0}$  states is also found. The experiments for the ratio of the partial decay width of  $X(3872)$  in the  $D^0\bar{D}^{*0}$  channel to that of the  $J/\psi\pi^2$  channel,  $r_{D^0\bar{D}^{*0}}$ , however, are still controversial: the Belle results give  $8.92 \pm 2.42$  for this value [7, 10] while the *BABAR* results give  $19.9 \pm 8.05$  [11, 12]. Here we cite the data only from the charged  $B$  decays because the  $X(3872)$  peak in the neutral  $B$  decay is still vague.

Let us mention another exceptional feature of the  $X(3872)$ , which we will discuss in this paper extensively. It is found that the  $X(3872)$  decays both to the  $J/\psi\rho$  and to the  $J/\psi\omega$  states. According to the experiments [13, 14], the decay fraction of  $X(3872)$  into two pions is comparable to that of three pions:

$$\begin{aligned} \frac{Br(X \rightarrow \pi^+\pi^-\pi^0 J/\psi)}{Br(X \rightarrow \pi^+\pi^- J/\psi)} &= 1.0 \pm 0.4 \pm 0.3 \quad (\text{Belle}) \\ &= 0.8 \pm 0.3 \quad (\text{BABAR}). \end{aligned} \tag{1}$$

This isospin mixing is very large comparing to the usual one. For example, the size of the breaking in the  $D^+-D^0$  mass difference is 0.003.

Many theoretical works are being reported since the first observation of  $X(3872)$ . From the lattice QCD approach, it has been reported that there is a level(s) in the  $1^{++}$  channel [15, 16]. Prelovsek *et.al.* investigated the  $1^{++}$  channel using various interpolators, and found the levels which correspond to the  $\chi_{c1}(1P)$ ,  $X(3872)$ , and the  $D\bar{D}^*$  scattering states [16]. It seems, however, that the present lattice calculation still has difficulty in dealing with a very shallow bound state or a resonance near the complicated thresholds with  $m_u \neq m_d$  yet. Most of the models for the  $X(3872)$  in the phenomenological approach can be classified into four types: a two-meson hadronic molecule, a  $c\bar{c}$  charmonium, a tetraquark, and the charmonium-two-meson hybrid state. Since the observed  $X(3872)$  mass is very close to the  $D^0\bar{D}^{*0}$  threshold, the possibility of  $X(3872)$  being the hadronic molecular structure has been widely discussed [17–33]. In order to explain the production rate of  $X(3872)$  in the high-energy  $p\bar{p}$  collisions experiments by the Tevatron and the LHC, however, a smaller object is favored. The charmonium options for the  $X(3872)$  has been carefully studied in refs. [34–36]. The diquark-antidiquark or the tetraquark structure of  $X(3872)$  has been studied in refs. [37–41]. The tetraquark state can be described by coupled two-meson states with the attraction arising from the quark degrees of freedom. So, as a model which has both of the above strong points, the charmonium-hadronic molecule hybrid structure has been proposed for  $X(3872)$  [42–54]. The production rates of  $X(3872)$  are one of the important observables and have been discussed in [55–63]. There are many experiments and theoretical studies on

**Table 1** The masses and widths of mesons and the  $X(3872)$  thresholds, and their energy difference (in MeV) [6].

$m_{D^0}$	$m_{D^{*0}}$	$m_{D^+}$	$m_{D^{*+}}$		
$1864.86 \pm 0.13$	$2006.99 \pm 0.15$	$1869.62 \pm 0.15$	$2010.29 \pm 0.13$		
$m_{J/\psi}$	$m_{\rho^0}$	$\Gamma_{\rho^0}$	$m_{\omega}$	$\Gamma_{\omega}$	
$3096.916 \pm 0.011$	$775.26 \pm 0.25$	$147.8 \pm 0.9$	$782.65 \pm 0.12$	$8.49 \pm 0.08$	
$m_{D^0} + m_{D^{*0}}$	$m_{J/\psi} + m_{\rho}$	$m_{J/\psi} + m_{\omega}$	$m_{D^+} + m_{D^{*+}}$	$m_{X(3872)}$	$\Gamma_{X(3872)}$
$3871.85 \pm 0.20$	$3872.18 \pm 0.25$	$3879.57 \pm 0.12$	$3879.91 \pm 0.20$	$3871.68 \pm 0.17$	$< 1.2$
-	0.33	7.72	8.06	-0.17	

the radiative decays [64–74]. The isospin symmetry breaking found in the  $X(3872)$  decay, Eqs. (1) and (2), is also discussed in various ways [43, 75–78].

As summarized in the review articles [79–81], it is difficult to explain the  $X(3872)$  properties by assuming a simple  $1^{++} c\bar{c}$  state. The spectrum of the final pions, the radiative decay, and the production rate suggest that the  $X(3872)$  is not just a meson molecule either. As seen in Table 1, there are four two-meson thresholds which are very close to the  $X(3872)$  mass. It is considered that  $X(3872)$  has a large amount of components of these two-meson states. Also, there is supposed to be a  $c\bar{c}(2P)$  state nearby, whose quantum number is the same as that of  $X(3872)$ ; the existence of  $c\bar{c}(2P)$  at 3950 MeV was predicted by the quark model which reproduces the meson masses below the open charm threshold very accurately [82]. It is also natural to assume that  $X(3872)$  has this  $c\bar{c}(2P)$  component.

As discussed in ref. [54, 78], and like many of the works mentioned above, we argue that the  $X(3872)$  is a hybrid state of the  $c\bar{c}$  and the two-meson molecule, a superposition of a  $D\bar{D}^*$  molecular state and the  $c\bar{c}(2P)$  quarkonium. There we found that  $X(3872)$  can be a shallow bound state (or an  $S$ -wave virtual state) and has an about 6%  $c\bar{c}$  charmonium component. The model assumes that the  $D\bar{D}^*$  channel has an attractive force between the two mesons. The size of this attraction is determined so that it produces a zero-energy resonance if the attraction of the same size is introduced in the  $B\bar{B}^*$  system. Namely, we assumed the maximum attraction which is consistent with the fact that no  $B\bar{B}^*$  bound state has been found yet. This attraction does not produce a bound state in the  $D\bar{D}^*$  system by itself because the reduced mass is much smaller. We introduce the coupling between the  $D\bar{D}^*$  and the charmonium,  $c\bar{c}(2P)$ , which gives the required extra attraction to make a bound state of the observed binding energy, 0.17 MeV. It has been found that this picture explains many of the observed properties of the  $X(3872)$ : the production rate of  $X(3872)$  in the  $p\bar{p}$  collision is about 1/20 of that of  $J/\psi$ , absence of the charged  $X$  which decays into  $J/\psi\rho^\pm$ , and a lack of the  $\chi_{c1}(2P)$  peak above the open charm threshold in the  $I(J^{PC}) = 0(1^{++})$  spectrum, whose existence was predicted by the quark model [54].

---

In this work, we investigate the  $D^0\overline{D}^{*0}$ ,  $D^+D^{*-}$ ,  $J/\psi\rho$ ,  $J/\psi\omega$  mass spectra observed in the  $B$  decay, especially the peak shape, the relative strength of each channel, and the size of the isospin symmetry breaking seen in Eqs. (1) and (2). For this purpose, we employ the hadron model explained above and introduce the  $J/\psi\rho$  and  $J/\psi\omega$  channels (denoted by the  $J/\psi V$  channels in the following) into the two-meson states in addition to  $D^0\overline{D}^{*0}$  and  $D^+D^{*-}$ . We take account of the energy dependent decay widths of the  $\rho$  and  $\omega$  mesons when we calculate the mass spectra. The  $D^*$  mesons also decay to  $D\pi$  or to  $D\gamma$  and have a width. We do not take their width into account, however, because they are much smaller than the width of the  $\rho$  and  $\omega$  mesons:  $96 \pm 22$  keV for  $D^{*+}$ (2010) and less than 2.1 MeV for  $D^{*0}$ (2007). The widths of the light vector mesons, especially the  $\rho$  meson, are very large comparing to the  $X(3872)$  width. We investigate the mechanism how these large widths give rise to the very narrow peak of  $X(3872)$ . We assume that the source of  $X(3872)$  is the  $c\overline{c}(2P)$  state, which is created from the  $B$  meson by the weak decay as  $B \rightarrow c\overline{c} + K$ . We take only the  $c\overline{c}(2P)$ , and not  $c\overline{c}(1P)$  for example, as the source or the component of  $X(3872)$  because this  $c\overline{c}(2P)$  state has the closest mass to the  $X(3872)$  among the  $J^{PC} = 1^{++}$   $c\overline{c}$  series calculated by the quark model. This situation may change when one investigates the radiative decay because each  $c\overline{c}$  core decays differently to the final  $J/\psi\gamma$  or  $\psi'\gamma$  states [74]. In this article, however, we discuss the hadronic decay and neglect the other  $c\overline{c}$  states because the mass spectrum does not change much if the  $c\overline{c}(1P)$  state is introduced [54]. A part of this work is discussed in [78].

The method we use is solving the Lippmann-Schwinger equation (LS equation) for the coupled-channel two-meson scattering problem with a bound state ( $c\overline{c}$ ) embedded in the continuum (BSEC) [83]. The energy-dependent  $\rho$  and  $\omega$  widths are included in each of the  $J/\psi V$  propagators. The isospin symmetry breaking in the present model originates from the difference in the charged and neutral  $D^{(*)}$  meson masses. Once the symmetry breaking occurs, the size of the breaking in the decay process is enhanced by the difference in the  $\rho$  and  $\omega$  meson widths. As mentioned above, the sources of the isospin symmetry breaking in  $X(3872)$  has been discussed in the literature: the kinetic factor which enhances the isospin  $I = 1$  component is discussed in ref. [43], the contribution from the  $\rho^0$ - $\omega$  mixing is pointed out in ref. [75], an estimate by a two-meson model with the realistic meson masses and the widths is reported in ref. [76], the isospin breaking in the one-boson exchange interaction is investigated in ref. [77]. Our approach is unique in the sense that (1) we calculated the mass spectrum against the energy of the  $D^0\overline{D}^{*0}$  final state up to 4 GeV, (2) the  $X(3872)$  peak is investigated according to the final branching fractions, (3) the energy dependent  $\rho$  and  $\omega$  meson widths are introduced, (4) the interaction between the  $D\overline{D}^*$  and the  $J/\psi V$  channels is determined from the quark model, and (5) the interaction between the  $D$  and

---

$\overline{D}^*$  is determined on the basis of the experiments that no  $B\overline{B}^*$  bound state has been found yet.

As we will discuss later in section 3, we found that the transfer strength from the  $c\bar{c}$  state to the  $J/\psi\rho$  or  $J/\psi\omega$  has a peak with a very narrow width below or on the  $D^0\overline{D}^{*0}$  threshold. The calculated size of the  $J/\psi\pi^3$  peak is 1.29-2.38 times as large as that of the  $J/\psi\pi^2$  peak. The large width of the  $\rho$  meson enhances the  $J/\psi\rho$  component in the decay mass spectrum and therefore decreases the ratio of the  $J/\psi\pi^3$  to the  $J/\psi\pi^2$ ,  $R_\Gamma$  from 12.4 to 1.29-2.38. Experimentally, this ratio corresponds to Eqs. (1) and (2). The value we have obtained is somewhat larger than the experiments, but much closer than the result without this enhancement. Moreover, we look into the parameter dependence of various ratios of the decay fractions. The ratio  $R_\Gamma$  become smaller as the size of the  $c\bar{c}-D\overline{D}^*$  coupling becomes smaller. The present experiments suggest that the about one-third of the attraction in  $X(3872)$  comes from this coupling. The relative strength of  $D^+D^{*-}$  to  $D^0\overline{D}^{*0}$  is also closely related to the size of the coupling. With these two observables combined, one may extract the condition over the size of interaction among the heavy quark systems. The ratio  $r_{D^0\overline{D}^{*0}}$  reflects the binding energy of the  $X(3872)$  rather strongly. It will help to understand the  $X(3872)$  state if this value is determined experimentally.

Recently, the  $Z_c(3900)^\pm$  resonance has been found in the  $J/\psi\pi^\pm$  mass spectrum [84, 85]. It is a charged charmonium-like state, which means that it is a genuine exotic state whose minimal quark component is  $c\bar{c}q\bar{q}$ . This model cannot be applied directly to the  $Z_c(3900)^\pm$  resonance; the  $Z_c(3900)$  is not a simple  $I = 1$  counter part of  $X(3872)$ . The system consists of two mesons (or more) and the resonance appears without the attraction from the  $c\bar{c}$ -two-meson coupling. There is a report that the peak may not be a resonance but a threshold effect [86]. Further works will be necessary to understand the  $Z_c(3900)^\pm$  resonance. For the charged bottomonium-like resonances,  $Z_b(10610)^\pm$  and  $Z_b(10650)^\pm$  [87], the present model cannot be applied directly, either, because these states again have a nonzero charge and do not couple to the bottomonium states. The  $Z_b(10610)^0$  resonance observed in  $\Upsilon(10860) \rightarrow \Upsilon(2,3S)\pi^0\pi^0$  decays [88] is probably be the neutral partner of  $Z_b(10610)^\pm$ , the  $I = 1$  state. The masses of the charged and the neutral  $Z_b(10610)$ 's are essentially the same, which means that the isospin symmetry breaking of this system is small. Thus, the coupling between the  $Z_b(10610)^0$  and the  $b\bar{b}$  state is also expected to be small. But it supports our idea that there can be an attraction between the  $Q\bar{Q}$  mesons as the existence of the  $Z_b$  resonance strongly suggests.

Among the heavy quarkonia,  $X(3872)$  seems a very interesting object in a sense that the relevant two-meson threshold(s) exist closely below the  $Q\bar{Q}$  state.  $X(3872)$  has an advantage that the state is well investigated both from the experimentally and theoretically. In this article, we focus our attention to  $X(3872)$  and discuss the other resonances elsewhere. The study of the  $X(3872)$ , however, gives us the information of the size of the interaction between

$D$  and  $\bar{D}^*$ , and therefore that between  $B$  and  $\bar{B}^*$  through the heavy quark symmetry. That helps us to understand the structures of these genuine exotic charmonium-like and bottomonium-like states. The results also gives us the information on the  $c\bar{c}$ - $D\bar{D}^*$  coupling, which is a clue to understand the light  $q\bar{q}$  pair creation and annihilation processes.

We will discuss the method in section 2. The results are given in section 3, and the summary is given in section 4.

## 2. Method

### 2.1. Model Space and Model Hamiltonian

Our picture of  $X(3872)$  is a superposition of the two-meson state and the  $c\bar{c}$  quarkonium. The two-meson state consists of the  $D^0\bar{D}^{*0}$ ,  $D^+D^{*-}$ ,  $J/\psi\omega$ , and  $J/\psi\rho$  channels. The  $c\bar{c}$  quarkonium, which couples to the  $D\bar{D}^*$  channels, is treated as a bound state embedded in the continuum (BSEC) [83, 89]. In the following formulae, we denote the two-meson state by  $P$ , and the  $c\bar{c}$  quarkonium by  $Q$ .

The wave function is written as

$$\Psi = \sum_{i=1}^4 c_i \psi_i^{(P)} + c_0 \psi^{(Q)} . \quad (3)$$

We assume that the state is  $J^{PC} = 1^{++}$ , but do not specify the isospin. The wave function of each two-meson channel in the particle basis is

$$\psi_1^{(P)} = \frac{1}{\sqrt{2}}(D^0\bar{D}^{*0} + D^{*0}\bar{D}^0) \quad (4)$$

$$\psi_2^{(P)} = \frac{1}{\sqrt{2}}(D^+D^{*-} + D^{*-}D^+) \quad (5)$$

$$\psi_3^{(P)} = J/\psi \omega \quad (6)$$

$$\psi_4^{(P)} = J/\psi \rho . \quad (7)$$

The model hamiltonian,  $H = H_0 + V$ , can be written as:

$$H = \begin{pmatrix} H^{(P)} & V_{PQ} \\ V_{QP} & E_0^{(Q)} \end{pmatrix} \quad (8)$$

with

$$H_0 = \begin{pmatrix} H_0^{(P)} & 0 \\ 0 & E_0^{(Q)} \end{pmatrix} \quad \text{and} \quad V = \begin{pmatrix} V_P & V_{PQ} \\ V_{QP} & 0 \end{pmatrix} , \quad (9)$$

where  $H^{(P)}$  is the Hamiltonian for the two-meson systems,  $V_{PQ}$  and  $V_{QP}$  are the transfer potentials between the two-meson systems and the  $c\bar{c}$  quarkonium.  $E_0^{(Q)}$  is a  $c$ -number and corresponds to the BSEC mass before the coupling to the  $P$ -space is switched on.

Since the concerning particles are rather heavy and the energy region is very close to the threshold, the nonrelativistic treatment is enough for this problem. For the free hamiltonian

**Table 2** Model parameters for the interaction. The interaction strength,  $v$ ,  $v'$ ,  $u$ , and  $g$ , are defined by Eq. (13). The  $g_0 = 0.04842$  is the strength of the  $c\bar{c}-D\bar{D}^*$  coupling which gives the correct  $X(3872)$  mass when  $v = v' = 0$ , and  $u = 0.1929$ . (See text.) For all the parameter sets,  $\Lambda = 500$  MeV, and  $E_0^{(Q)} = 3950$  MeV.

	$v$	$v'$	$u$	$g$	$(g/g_0)^2$
A	-0.1886	0	0.1929	0.03933	0.66
B	-0.2829	0	0.1929	0.03356	0.48
C	-0.1886	0	0.2894	0.03424	0.50
QM	0.0233	-0.2791	0.1929	0.04850	1.00

for the  $P$ -space, we have

$$H_0^{(P)} = \sum_i \left( M_i + m_i + \frac{k_i^2}{2\mu_i} \right), \quad (10)$$

where  $M_i$  and  $m_i$  are the masses of the two mesons of the  $i$ -th channel,  $\mu_i$  is their reduced mass,  $k_i$  is their relative momentum. Because of the same reason, the system will not depend much on the details of the interaction. So, we employ a separable potential for the interaction between the two mesons,  $V_P$ . The potential  $V_P$  between the  $i$ th and  $j$ th channels is written as

$$V_{P;ij}(\mathbf{p}, \mathbf{p}') = v_{ij} f_\Lambda(p) f_\Lambda(p') Y_{00}(\Omega_p) Y_{00}^*(\Omega_{p'}) \quad \text{with} \quad f_\Lambda(p) = \frac{1}{\Lambda} \frac{\Lambda^2}{p^2 + \Lambda^2}, \quad (11)$$

where  $v_{ij}$  is the strength of the two-meson interaction. We use a typical hadron size for the value of the cutoff,  $\Lambda$ , and use the same value for all the channels. The transfer potential  $V_{QP}$  between the  $Q$  space and the  $i$ th channel of the  $P$  space is taken to be

$$V_{QP;i}(\mathbf{p}) = g_i \sqrt{\Lambda} f_\Lambda(p) Y_{00}^*(\Omega_p), \quad (12)$$

where the factor  $g_i$  stands for the strength of the transfer potential. We use the same function,  $f_\Lambda$ , also for the  $V_{PQ}$  for the sake of simplicity.

The channel dependence of  $v_{ij}$  and  $g_i$  is assumed to be

$$\{v_{ij}\} = \begin{Bmatrix} v & 0 & u & u \\ 0 & v & u & -u \\ u & u & v' & 0 \\ u & -u & 0 & v' \end{Bmatrix} \quad \text{and} \quad \{g_i\} = \begin{Bmatrix} g & g & 0 & 0 \end{Bmatrix} \quad (13)$$

for the  $D^0\bar{D}^{*0}$ ,  $D^+D^{*-}$ ,  $J/\psi\omega$ , and  $J/\psi\rho$  channels, respectively.

As for the size of the attraction between the two mesons, we have tried four sets of parameters, A, B, C and QM. The parameters of each parameter set are listed in Table 2. The following assumptions are common to all the parameter sets: (1) the attraction in the  $D^0\bar{D}^{*0}$  channel is the same as that of  $D^+D^{*-}$ , (2) there is no direct mixing between these  $D^0\bar{D}^{*0}$  and  $D^+D^{*-}$  channels, (3) the interaction between the  $J/\psi$  and the  $\omega$  meson is the same as

that of the  $J/\psi$  and the  $\rho$  meson, and (4) there is no transfer potential between the two  $J/\psi V$  channels. These assumptions mean that the interaction between the two mesons in the  $I(J^{PC}) = 1(1^{++})$  state is the same as that of  $0(1^{++})$ . The interaction strength in the  $J/\psi V$  channels,  $v'$ , however, can be different from the one for the  $D\bar{D}^*$  channels,  $v$ . The size of the coupling between the  $D\bar{D}^*$  and the  $J/\psi V$  channels,  $u$ , is derived from the quark model, which we will explain later in this section.

As for the  $c\bar{c}$  quarkonium mass,  $E_0^{(Q)}$ , we use the  $\chi_{c1}(2P)$  mass obtained by the quark model [82]. As for the strength of the transfer potential,  $\{g_i\}$ , we assume that  $D^0\bar{D}^{*0}$  and  $D^+D^{*-}$  couple to the  $c\bar{c}$  quarkonium directly whereas the  $J/\psi V$  channels do not. It is because the former coupling occurs by the one-gluon exchange while the latter coupling is considered to be small because of the OZI rule. Since the annihilation terms which cause the  $c\bar{c}$ - $D^0\bar{D}^{*0}$  and  $c\bar{c}$ - $D^+D^{*-}$  couplings are considered to be the same, we assume these two channels have the same  $g$ . The  $g$  is taken as a free parameter in each parameter set to reproduce the  $X(3872)$  peak at the observed energy.

Suppose both of  $v$  and  $v'$  are equal to zero, the coupling  $g$  has to be 0.04842 to give the correct  $X(3872)$  mass, which we denote  $g_0$  in the following. The rough size of the  $c\bar{c}$  quarkonium contribution to the attraction to bind the  $X(3872)$  can be expressed by  $(g/g_0)^2$ . When  $(g/g_0)^2$  is close to 1, the attraction comes mainly from the  $c\bar{c}$ - $D\bar{D}^*$  coupling, whereas the attraction comes largely from the two-meson interaction when  $(g/g_0)^2$  is smaller. The size of  $g_0$  in the present work is somewhat smaller than but not very different from the corresponding value in the previous work, 0.05110, where the  $J/\psi V$  channels were not introduced yet [54]. It seems that the effect of the  $J/\psi V$  channels on the  $X(3872)$  mass is not large. As we will show later, its effect on the transfer spectrum in the higher energy region is not large, either. Introducing the  $J/\psi V$  channels, however, changes the phenomena at the  $D^0\bar{D}^{*0}$  threshold drastically.

For a single channel problem with the Lorentzian separable interaction, the binding energy,  $E_B$ , can be obtained analytically:

$$-v\mu = \frac{(\alpha + \Lambda)^2}{\Lambda} \quad \text{with} \quad \alpha = \sqrt{2\mu E_B}. \quad (14)$$

For the  $B^0\bar{B}^{*0}$  system, the condition to have a bound state is  $v < -0.1886$  with  $\Lambda = 500$  MeV. In the parameter set A, we assume this value,  $-0.1886$ , for the strength of the interaction between the  $D$  and  $\bar{D}^*$  mesons. Namely, the  $D\bar{D}^*$  attraction is taken as large as possible on condition that there is a zero-energy resonance but no bound state in the  $B^0\bar{B}^{*0}$  systems if the attraction of the same size is applied [54]. Since it requires  $v < -0.5172$  for the  $D^0\bar{D}^{*0}$  channel to have a bound state only by the  $D^0\bar{D}^{*0}$  attraction, this assumption means that here we assume only 0.36 of the required attraction comes from the  $D^0\bar{D}^{*0}$  diagonal part. We also assume that the interaction between  $J/\psi$  and  $\rho$  or  $J/\psi$  and  $\omega$  is taken to be zero,  $v' = 0$ , for the parameter set A.

In the parameter set B [C], we use  $v$  [ $u$ ] 1.5 times as large as that of the parameter set A to see the parameter dependence. We use the one from the quark model also for the diagonal part,  $v$  and  $v'$ , in the parameter set QM.

We have introduced the width into the  $J/\psi V$  channels, which represents the decays to  $J/\psi \pi^n$ . In the present model, the source of the isospin symmetry breaking is the charged and neutral  $D^{(*)}$  meson mass difference. The couplings and the two-meson interactions mentioned above conserve the isospin symmetry.

## 2.2. The Lippmann-Schwinger equation and the transfer strength

We solve the Lippmann-Schwinger (LS) equation to investigate the  $X(3872)$ . Let us show some of its formulae for the case with the BSEC. The LS equation for the  $T$ -matrix and the full propagator  $G$  can be written as

$$T = V + VG_0T \quad (15)$$

$$G = G_0 + G_0VG = G_0 + GVG_0 \quad (16)$$

with

$$G_0 = (E - H_0 + i\epsilon)^{-1} = \mathcal{P}(E - H_0)^{-1} - i\pi\delta(E - H_0) \quad (17)$$

$$G = (E - H + i\epsilon)^{-1} , \quad (18)$$

where  $\mathcal{P}$  indicates that the principal value should be taken for the integration of this term.

Suppose there is no  $Q$ -space, then the ‘full’ propagator solved within the  $P$ -space,  $G^{(P)}$ , can be obtained as

$$G^{(P)} = (E - H_P + i\epsilon)^{-1} \quad (19)$$

$$= G_0^{(P)} \left( 1 + V_P G^{(P)} \right) = \left( 1 + G^{(P)} V_P \right) G_0^{(P)} . \quad (20)$$

When the coupling to the  $Q$ -space is introduced, the full propagator for that state becomes

$$G_Q = \left( E - E_Q^{(0)} - \Sigma_Q \right)^{-1} , \quad (21)$$

where  $\Sigma_Q$  is the self energy of the  $Q$ -space,

$$\Sigma_Q = V_{QP} G^{(P)} V_{PQ} . \quad (22)$$

Since  $\Sigma_Q$  is the only term which has an imaginary part in  $G_Q$ , we have

$$\text{Im } G_Q = \text{Im } G_Q^* \Sigma_Q G_Q \quad (23)$$

$$= \text{Im } G_Q^* V_{QP} G^{(P)} V_{PQ} G_Q \quad (24)$$

$$= \text{Im } G_Q^* V_{QP} G^{(P)} G^{(P)*-1} G^{(P)*} V_{PQ} G_Q . \quad (25)$$

Using  $\text{Im } G^{(P)*-1} = \text{Im } G_0^{(P)*-1}$  and Eq. (20), the above equation can be rewritten as

$$\text{Im } G_Q = \text{Im } G_Q^* V_{QP} (1 + G^{(P)} V_P) G_0^{(P)} (1 + V_P G^{(P)*}) V_{PQ} G_Q . \quad (26)$$

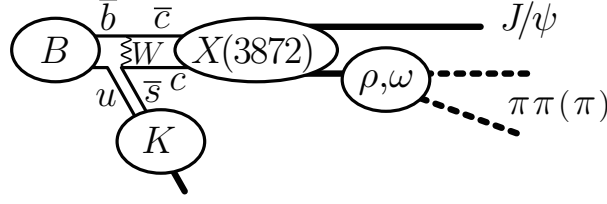


**Fig. 1** The  $X(3872)$  formation process with the final  $J/\psi V$  channel in the  $B$  meson decay.

In the actual calculation we use the following relation with the  $T$ -matrix within the  $P$ -space,  $T^{(P)}$ ,

$$V_P G^{(P)} = T^{(P)} G_0^{(P)}, \quad G^{(P)} V_P = G_0^{(P)} T^{(P)} \quad (27)$$

$$T^{(P)} = \left(1 - V_P G_0^{(P)}\right)^{-1} V_P. \quad (28)$$

It is considered that the  $X(3872)$  state is produced via the  $c\bar{c}$  quarkonium (Fig. 1). Thus the transfer strength from the  $c\bar{c}$  quarkonium to the final meson states corresponds to the observed mass spectrum with a certain factor of the weak interaction as well as the formation factor of the  $c\bar{c}$  quarkonium, which we do not consider in this work. In the following, we explain how we calculate the transfer strength. Notations of the kinematics are summarized in Appendix A.1.

First, we derive the strength without the  $\rho$  or  $\omega$  meson widths. The transfer strength from the  $c\bar{c}$  to the two-meson state,  $W$ , becomes

$$\frac{dW}{dE} = -\frac{1}{\pi} \text{Im} \langle c\bar{c} | G_Q | c\bar{c} \rangle, \quad (29)$$

where  $E$  is the energy of the system when the center of mass of  $D^0 \bar{D}^{*0}$  is at rest. In order to obtain the strength to each final two-meson state separately, we rewrite the Eq. (29) as

$$\begin{aligned} \frac{dW}{dE} &= -\frac{1}{\pi} \text{Im} \langle c\bar{c} | G_Q^* V_{QP} (1 + G^{(P)} V_P) G_0^{(P)} (1 + V_P G^{(P)*}) V_{PQ} G_Q | c\bar{c} \rangle \\ &= -\frac{1}{\pi} \text{Im} \sum_f \int d^3 \mathbf{k} \langle f; \mathbf{k} | G_0^{(P)}(E) | f; \mathbf{k} \rangle \left| \langle f; \mathbf{k} | (1 + V_P G^{(P)*}) V_{PQ} G_Q | c\bar{c} \rangle \right|^2, \end{aligned} \quad (30)$$

where the summation is taken over all the final two-meson channels,  $f$ , with the momentum  $\mathbf{k}$ , which is denoted by  $|f; \mathbf{k}\rangle$ . Eq. (31) is derived by using the fact that the imaginary part of rhs of Eq. (30) arises only from the imaginary part of  $G_0^{(P)}$  in the middle of the matrix element. The free propagator  $G_0^{(P)}$  can be rewritten as

$$\langle f; \mathbf{k} | G_0^{(P)}(E) | f; \mathbf{k} \rangle = \frac{1}{E - (M_f + m_f + \frac{k^2}{2\mu_f}) + i\epsilon} = \frac{2\mu_i}{k_f^2 - k^2 + i\epsilon} \quad (32)$$

$$= 2\mu_f \frac{\mathcal{P}}{k_f^2 - k^2} - i\pi\mu_f \frac{\delta(k - k_f)}{k_f}, \quad (33)$$

where the  $k_f$  is the size of the relative momentum of the two meson system in the  $f$ th channel,  $E = M_f + m_f + k_f^2/(2\mu_f)$ . Thus we have the strength for the open channel  $f$  as

$$\frac{dW(c\bar{c} \rightarrow f)}{dE} = \mu_f k_f \left| \langle f; k_f | (1 + V_P G^{(P)*}) V_{PQ} G_Q | c\bar{c} \rangle \right|^2. \quad (34)$$

Next, we introduce the decay widths. For this purpose, we modify the free propagator in the  $P$ -space,  $G_0^{(P)}$ , as

$$\langle f; k | G_0^{(P)}(E) | f; k \rangle \rightarrow \langle f; k | \tilde{G}_0^{(P)}(E) | f; k \rangle = \left( E - H_0^{(P)} + \frac{i}{2} \Gamma_V \right)^{-1}. \quad (35)$$

The width comes from the imaginary part of the self energy of the  $\rho$  or  $\omega$  mesons which couple to the  $\pi^n$  states. The real part of the self energy is taken care of by using the observed masses in the denominator. The width of the mesons,  $\Gamma_V$ , depends on the energy of the  $n\pi$  final state,  $E_{n\pi}$ . We use the energy dependent decay width which produces the observed  $\rho$  or  $\omega$  width (see Appendix A.2).

By the above substitution, the full propagator,  $G^{(P)}$  and  $G_Q$ , the self energy  $\Sigma_Q$  are also modified as

$$\tilde{G}^{(P)} = \left( E - H^{(P)} + \frac{i}{2} \Gamma_V \right)^{-1} = \tilde{G}_0^{(P)} (1 - V_{PP} \tilde{G}_0^{(P)})^{-1} \quad (36)$$

$$\tilde{\Sigma}_Q = V_{QP} \tilde{G}^{(P)} V_{PQ} \quad (37)$$

$$\tilde{G}_Q = \left( E - E_Q^{(0)} - \tilde{\Sigma}_Q \right)^{-1}. \quad (38)$$

Thus the strength for the open channel  $f$  becomes

$$\frac{dW(c\bar{c} \rightarrow f)}{dE} = \frac{2}{\pi} \mu_f \int \frac{k^2 dk}{(k_f^2 - k^2)^2 + (\mu_f \Gamma_f)^2} \left| \langle f; k | (1 + V_P \tilde{G}^{(P)*}) V_{PQ} \tilde{G}_Q | c\bar{c} \rangle \right|^2. \quad (39)$$

$\Gamma_f$  is the width of the  $f$ th channel. The width of the  $J/\psi V$  channels depend both on  $k$  and on  $k_f$  through  $E_{n\pi}$ . The above strength is normalized as

$$\sum_f \int_0^\infty dE \frac{dW(c\bar{c} \rightarrow f)}{dE} = 1 \quad (40)$$

when finite, energy-independent widths are employed. When the widths become energy dependent, the above integral changes to, for example, 0.988 for the parameter set A.

In order to see the mechanism to have a peak, we factorize the transfer strength as

$$\frac{dW(c\bar{c} \rightarrow f)}{dE} = \Delta_f(E) D_{PQ}(E) |\langle c\bar{c} | \tilde{G}_Q(E) | c\bar{c} \rangle|^2 \quad (41)$$

$$\Delta_f(E) = \frac{2}{\pi} \int \frac{k^2 dk}{(k_f^2 - k^2)^2 + (\mu_f \Gamma_f)^2} \frac{f_\Lambda(k)^2}{f_\Lambda(k_f)^2} \quad (42)$$

$$D_{PQ}(E) = \mu_f \left| \langle f; k_f | (1 + V_P \tilde{G}^{(P)*}) V_{PQ} | c\bar{c} \rangle \right|^2, \quad (43)$$

where  $\Delta_f(E) \rightarrow k_f$  as  $\Gamma_f \rightarrow 0$ . For the energy around the  $D^0 \bar{D}^{*0}$  threshold, the integrand of the factor  $\Delta_{J/\psi\rho}(E)$  has the maximum at around  $k \sim 1.26$  fm, which corresponds to  $E_{2\pi} \sim$

670 MeV. There,  $\Gamma_{J/\psi\rho}$  is 0.89 times as large as that of the energy independent value, 149.1 MeV. On the other hand, since the  $\omega$  meson width is much smaller than that of  $\rho$  meson,  $E_{3\pi}$  which gives main contribution is much closer to the peak:  $E_{3\pi} \sim 762$  MeV. There, the width also reduces to 0.89 times of the energy independent value 8.49 MeV. Since the out-going wave function solved in the  $P$  space,  $|f; k_f\rangle$ , can be expressed by the plane wave as  $|f; k_f\rangle = (1 + G^{(P)}V_P)|f; k_f\rangle$ , the  $D_{PQ}$  term is considered as the transfer probability between the  $P$ - and the  $Q$ -space,  $\mu_f |\langle f; k_f | V_{PQ} | c\bar{c} \rangle|^2$ .

### 2.3. The $J/\psi\omega$ - and $J/\psi\rho-D\bar{D}^*$ transfer potential from the quark model

In this subsection we explain how we obtain the transfer potential between the  $J/\psi\omega$ - and  $J/\psi\rho-D\bar{D}^*$  channels from a quark model. For this purpose, we employ the model of ref. [82], where they found the  $q\bar{q}$  meson masses as well as their decays are reproduced reasonably well. Since the results of the present work do not depend much on the model detail as we will show later, we simplify the quark model in order to apply it to multiquark systems as follows: (1) we remove the smearing from the gluonic interaction, (2) we remove the momentum dependence of the strong coupling constant ( $\alpha_s$ ) but let it depend on the flavors of the interacting quarks, (3) we only use a single gaussian orbital configuration for each mesons, each of whose size parameters corresponds to the matter root mean square radius ( $rms$ ) of the original model solved without the spin-spin term, and (4) we remove the energy dependence from the spin-spin term and multiply the term by a parameter ( $\xi$ ) to give a correct hyperfine splitting.

The quark hamiltonian consists of the kinetic term,  $K_q$ , the confinement term,  $V_{\text{conf}}$ , the color-Coulomb term,  $V_{\text{coul}}$ , and color-magnetic term,  $V_{\text{CMI}}$ :

$$H_q = K_q + V_{\text{conf}} + V_{\text{coul}} + V_{\text{CMI}} \quad (44)$$

$$K_q = \sum_i K_i \quad \text{with } K_i = \sqrt{m_i^2 + p_i^2} \quad (45)$$

$$V_{\text{coul}} = \sum_{i < j} \frac{(\lambda_i \cdot \lambda_j) \alpha_{sij}}{4 r_{ij}} \quad (46)$$

$$V_{\text{conf}} = \sum_{i < j} \frac{(\lambda_i \cdot \lambda_j)}{4} \left( -\frac{4}{3} \right)^{-1} (b r_{ij} + c) \quad (47)$$

$$V_{\text{CMI}} = - \sum_{i < j} \frac{(\lambda_i \cdot \lambda_j)}{4} (\sigma_i \cdot \sigma_j) \frac{2\pi}{3} \alpha_{sij} \frac{\xi_{ij}}{m_i m_j} \delta^3(r_{ij}) , \quad (48)$$

where  $m_i$  and  $p_i$  are the  $i$ th quark mass and momentum, respectively,  $r_{ij}$  is the relative distance between the  $i$ th and  $j$ th quarks,  $\alpha_{sij}$  is the strong coupling constant which depends on the flavor of the interacting the  $i$ th and  $j$ th quarks,  $b$  is the string tension,  $c$  is the overall shift.

**Table 3** Quark model parameters. The  $u$  and  $c$  quark masses,  $m_u$  and  $m_c$ , the string tension  $b$  and the overall shift  $c$  are taken from ref. [82]. As for the  $\alpha_s$ ,  $\xi$  and  $\beta$ , see text.

$m_u(\text{MeV})$	$m_c(\text{MeV})$	$b(\text{GeV}^2)$	$c(\text{MeV})$
220	1628	0.18	-253
	$\alpha_s$	$\xi$	$\beta(\text{fm})$
$u\bar{u}$	0.9737	0.1238	0.4216
$u\bar{c}, \bar{u}c$ or $uc$	0.6920	0.2386	0.3684
$c\bar{c}$	0.5947	0.5883	0.2619

**Table 4** Meson masses and the components of the quark potentials. All entries are in MeV.  $\langle K \rangle$ ,  $\langle V_{\text{coul}} \rangle$ ,  $\langle V_{\text{conf}} \rangle$ , and  $\langle V_{\text{CMI}} \rangle$  are the expectation values of the kinetic, the color-Coulomb, the confinement, and the color-magnetic terms, respectively.  $M_0$  is the summation of the first three terms. The underlined entries are used for the fitting. The observed masses,  $M_{\text{obs}}$ , (and the hyperfine splitting,  $hfs$ ,) are taken from ref. [6]. Since we fit the meson masses,  $M_{\text{obs}}$  is equal to  $\langle K \rangle + \langle V_{\text{coul}} \rangle + \langle V_{\text{conf}} \rangle + \langle V_{\text{CMI}} \rangle$ . The values in the parentheses are the results of the original model with no spin-spin interaction.

		$\langle K \rangle$	$\langle V_{\text{coul}} \rangle$	$\langle V_{\text{conf}} \rangle$	$M_0$	$\langle V_{\text{CMI}} \rangle$	$M_{\text{obs}}$	$hfs$
simplified	$D$	2402.9	-557.6	126.2	1971.5	-106.6	<u>1864.9</u>	142.1
	$D^*$	2402.9	-557.6	126.2	1971.5	35.5	<u>2007.0</u>	
	$\eta_c$	3726.1	-674.1	16.6	3068.6	-84.9	<u>2983.7</u>	113.2
	$J/\psi$	3726.1	-674.1	16.6	3068.6	28.3	<u>3096.9</u>	
	$\omega$	1159.2	-685.6	181.0	<u>654.6</u>	128.0	<u>782.7</u>	-
original	$\omega$	(1198.7)	(-721.0)	(176.9)	(654.6)		771.3	

The parameters are summarized in Table 3. The obtained meson masses and the components are listed in Table 4. We use the values for the quark masses and the confinement parameters,  $m_q$ ,  $b$ , and  $c$ , in ref. [82] as they are. Each  $q\bar{q}$  system has three other parameters:  $\alpha_s$ ,  $\xi$ , and the size parameter of the wave function,  $\beta$ . The values of  $\alpha_s$  and the  $\xi$  are taken so that the model gives the observed masses of the spin 0 and 1 mesons:  $D$ ,  $D^*$ ,  $\eta_c$ ,  $J/\psi$ ,  $\omega$  (the underlined entries in Table 4). We do not use the  $\eta$  meson mass for the fitting because the mass difference between  $\omega$  and its spin partner  $\eta$  cannot be considered as a simple hyperfine splitting. Instead, we use the  $\omega$  mass obtained from the original model without the spin-spin term,  $M_0$ , as a guide.

As seen in Table 3, the  $\alpha_s$  becomes smaller as the interacting quark masses become larger. The size parameter of the orbital gaussian is small for the  $c\bar{c}$  system, and larger for the  $u\bar{u}$  system. The factor for the CMI,  $\xi$ , varies widely from 0.1238 to 0.5883. These values, however, are reasonable because  $(\frac{m}{E})^2 \sim (\frac{m_u}{\langle K \rangle_\omega/2})^2 = 0.144$  and  $(\frac{m_c}{\langle K \rangle_{J/\psi}/2})^2 = 0.764$ . In the following, we will explain how we derive the potential between the hadrons from the quark model. The obtained potential, however, is mostly determined by the observables as seen

from Table 4. It does not depend much on the detail of the quark model, except for the color-spin dependence of the quark potential and the meson size parameters,  $\beta$ 's.

We use the following base functions to extract the two-meson interaction.

$$\psi_i^{(1)} = |\overline{D}_1 D^*_1\rangle \phi(\beta_{uc}, r_{14}) \phi(\beta_{uc}, r_{23}) \phi(\beta_i, r_{14-23}) \quad (49)$$

$$\psi_i^{(2)} = |V_1 J/\psi_1\rangle \phi(\beta_{uu}, r_{13}) \phi(\beta_{cc}, r_{24}) \phi(\beta_i, r_{13-24}) \quad (50)$$

$$\phi(\beta, r) = (\pi\beta^2)^{-3/4} \exp\left[-\frac{r^2}{2\beta^2}\right], \quad (51)$$

where  $|\overline{D}_1 D^*_1\rangle$  [ $|V_1 J/\psi_1\rangle$ ] corresponds to the spin-flavor-color part of the wave function in which the  $u\bar{c}$  [ $u\bar{u}$ ] quark pair is in the color singlet state (see appendix B). As for the orbital part, we use a single gaussian function for the internal meson wave function and gaussian base for the relative wave function of the two mesons. These base functions are not orthogonal to each other. Their normalization becomes

$$\mathcal{N} = \langle \psi_i^{(c)} | \psi_j^{(c')} \rangle = \begin{pmatrix} N & \frac{1}{3}\nu \\ \frac{1}{3}t\nu & N \end{pmatrix} \quad (52)$$

$$N_{ij} = \int 4\pi r^2 dr \phi(\beta_i, r) \phi(\beta_j, r) = \left( \frac{2\beta_i \beta_j}{\beta_i^2 + \beta_j^2} \right)^{3/2} \quad (53)$$

$$\nu_{ij} = \int \prod_{all\ r's} d\mathbf{r} \phi(\beta_{uc}, r_{14}) \phi(\beta_{uc}, r_{23}) \phi(\beta_i, r_{14-23}) \phi(\beta_{uu}, r_{13}) \phi(\beta_{cc}, r_{24}) \phi(\beta_j, r_{13-24}) . \quad (54)$$

The  $\nu$  vanishes as  $\mathcal{O}(\beta_i^{-3})$  when the  $\beta_i \sim \beta_j$  becomes large, whereas the  $N$  becomes one when  $\beta_i = \beta_j$ .

The normalization can be ‘diagonalized’ by

$$\mathcal{B} \mathcal{N}^t \mathcal{B} = \begin{pmatrix} N & 0 \\ 0 & N \end{pmatrix} \quad (55)$$

$$\mathcal{B} = \begin{pmatrix} \sqrt{N} \frac{1}{\sqrt{X}} & -\frac{1}{3} \sqrt{N} \frac{1}{\sqrt{X}} \nu \frac{1}{N} \\ 0 & 1 \end{pmatrix} \quad (56)$$

$$X = N - \frac{1}{9} \nu \frac{1}{N} t\nu . \quad (57)$$

The transfer matrix  $\mathcal{B}$  is not unique. We choose the above  $\mathcal{B}$  so that the base functions become  $|V_8 J/\psi_8\rangle$  and  $|V_1 J/\psi_1\rangle$  rather than  $|\overline{D}_1 D^*_1\rangle$  and  $|V_1 J/\psi_1\rangle$  at the short distance. By choosing this and by adding the width in the  $|V_1 J/\psi_1\rangle$  channel, we ensure that the  $\rho$  or  $\omega$  meson decay occurs just from the color-singlet light quark-antiquark pair and that the OZI rule can be applied to the  $VJ/\psi$  channel. Since the meson sizes are different from each other, the  $|\overline{D}_8 D^*_8\rangle$  and  $|V_8 J/\psi_8\rangle$  with orbital excitation can be introduced as additional base. We, however, do not take them into account for the sake of simplicity.

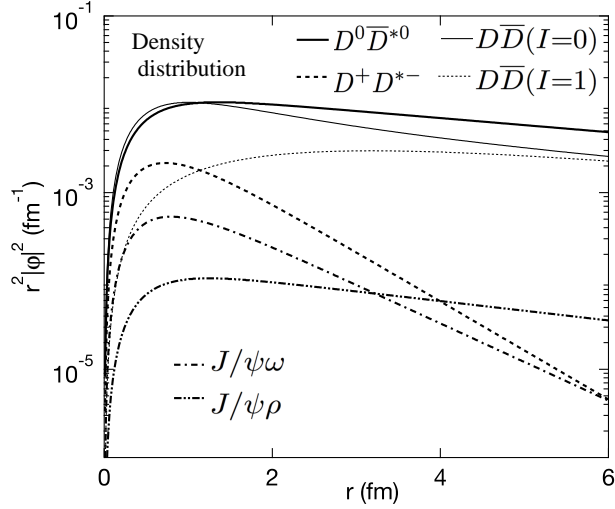


**Fig. 2** The density distribution of the  $X(3872)$  bound state against the relative distance of the two mesons,  $r$ , for the parameter set A calculated without introducing the meson decay width.

The hamiltonian for the two meson becomes

$$\mathcal{H} = \langle \psi_i^{(c)} | H_q | \psi_j^{(c')} \rangle \quad (58)$$

and one can extract the effective interaction for the  $\phi$  base as

$$\mathcal{V}^{\text{eff}} = \mathcal{B} \mathcal{H}^t \mathcal{B} - \begin{pmatrix} K_{\text{mesons}}^{(1)} & 0 \\ 0 & K_{\text{mesons}}^{(2)} \end{pmatrix} \quad (59)$$

$$K_{\text{mesons}}^{(c)} = \int 4\pi r^2 dr \phi(\beta_i, r) \left( \sqrt{m_c^2 + p^2} + \sqrt{M_c^2 + p^2} \right) \phi(\beta_j, r) . \quad (60)$$

We obtain the strength of the separable potential for the two-meson systems,  $V_P$ , so that their matrix elements calculated by the wave function of a very shallow bound state has the same value. Namely, we determine the values of  $u$ ,  $v$  and  $v'$  in the parameter set QM in Table 2 from the condition

$$\int \psi_\alpha V_P \psi_\alpha = \int \psi_\alpha \mathcal{V}^{\text{eff}} \psi_\alpha \quad \text{with} \quad \psi_\alpha(r) \propto \frac{e^{-\alpha r} - e^{-\Lambda r}}{r} , \quad (61)$$

where  $\psi_\alpha$  is the wave function for the separable potential in Eq. (14) for the state of the binding energy 1 MeV. The obtained value for  $u$  is used also for the parameter sets A and B.

### 3. Results and discussions

#### 3.1. The $X(3872)$ bound state

First we discuss the bound state which corresponds to  $X(3872)$ . In Fig. 2, the density distribution of the bound state for each two-meson channel versus the relative distance of the two mesons,  $r$ , is plotted for the parameter set A calculated without introducing the

**Table 5** Probabilities of each component in the  $X(3872)$  bound state calculated by the model without the meson width.

Model	$D^0\bar{D}^{*0}$	$D^+D^{*-}$	$J/\psi\omega$	$J/\psi\rho$	$c\bar{c}$
A	0.892	0.043	0.012	0.007	0.045
B	0.920	0.029	0.011	0.011	0.030
C	0.896	0.026	0.024	0.024	0.030
QM	0.834	0.060	0.023	0.008	0.075

meson width. The interaction range of the present model is  $\Lambda^{-1} \sim 0.4$  fm. The slope of the density distribution outside this range is essentially determined by the energy difference from each threshold. The size of the isospin  $I = 1$  component of  $D\bar{D}^*$  is small in the short range region. It, however, becomes the same amount as that of the  $I = 0$  component at the large distance because the  $D^+D^{*-}$  wave function decreases much faster than that of  $D^0\bar{D}^{*0}$ . The difference in the slopes of the  $J/\psi\omega$  and the  $J/\psi\rho$  densities also comes from the energy difference of their thresholds.

The largest component of  $X(3872)$  is  $D^0\bar{D}^{*0}$  because the lowest threshold is the  $D^0\bar{D}^{*0}$  and the binding energy is very small, 0.17 MeV. Though the  $J/\psi\rho$  threshold is similarly low, the size of its component in  $X(3872)$  is small. This can be explained because the  $J/\psi\rho$  system has a larger kinetic energy than the  $D\bar{D}^*$  does, but does not have enough attraction to make a state as low as  $D\bar{D}^*$  due to a lack of the coupling to  $c\bar{c}$ . The size of the  $J/\psi\omega$  component is somewhat larger than that of the  $J/\psi\rho$  at the short distance, because it is an  $I = 0$  channel.

In Table 5, we show the size of each component in the  $X(3872)$  bound state calculated by the present model without the meson width. The obtained size of the  $c\bar{c}$  component varies from 0.030 to 0.075 according to the parameters. The probability of the  $c\bar{c}$  component is 0.045 for the parameter set A, which is somewhat smaller, but similar to that of the  $(g/g_0)^2 \sim 0.5$  case in our previous work [54], where we investigated the  $X(3872)$  without the  $J/\psi V$  channels. This result is qualitatively supported by the experiment that the  $X(3872)$  production rate is about 1/20 of the  $J/\psi$  production rate in the  $p\bar{p}$  collision [90]. The idea of the parameter QM in the present work is similar to the model C in ref. [48], where the  $c\bar{c}(2P)$  is found to be 7%. Our result, 7.5%, is consistent with their result. Including the effective  $D\bar{D}^*$  attraction reduces the  $c\bar{c}$  probability as seen in Table 5 under the entries of the parameter set A-C.

It seems that the  $\rho$  and  $\omega$  components of the bound state are comparable in size. This does not directly mean that the  $\rho$  and  $\omega$  fraction from the  $X(3872)$  in the  $B$  decay are comparable. As we will show in the next subsection, the  $\omega$  fraction becomes larger because

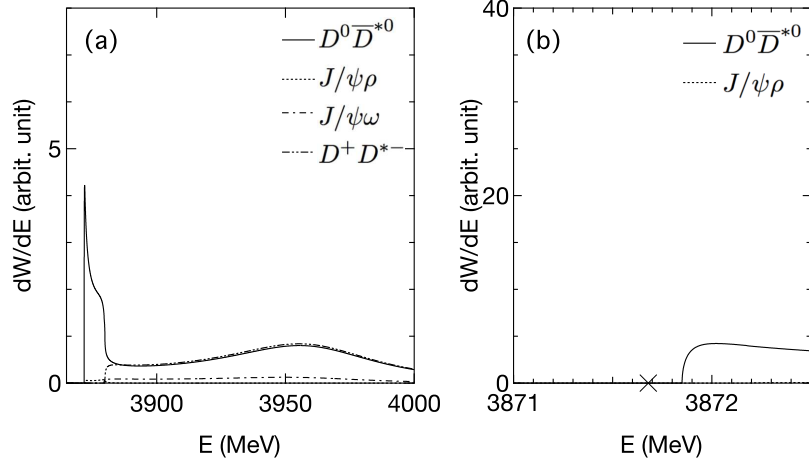


**Fig. 3** The transfer strength from the  $c\bar{c}$  quarkonium to the two-meson states (a) for  $3870 \text{ MeV} \leq E \leq 4000 \text{ MeV}$  and (b) around the  $D^0 \bar{D}^{*0}$  threshold. The spectra are for the parameter set A without the meson widths. The solid lines are for the transfer strength which goes from  $c\bar{c}$  into the  $D^0 \bar{D}^{*0}$  channel. Figs. (a) and (b) show the same spectra with a different scale both in the vertical and horizontal axes. In Fig. (b), the  $J/\psi\rho$  spectrum is shown but almost invisible in this scale, whereas the  $J/\psi\omega$  and  $D^+ D^{*-}$  spectra are not shown because the channels are not open in this energy region.

the formation of  $X(3872)$  occurs from the  $c\bar{c}$ , and the  $\rho$  fraction in turn is enhanced because of its large decay width.

### 3.2. The transfer strength from $c\bar{c}$ to the two-meson states

Next we discuss the transfer strength defined by eq. (29) from the  $c\bar{c}$  quarkonium to the final two-meson states,  $D^0 \bar{D}^{*0}$ ,  $D^+ D^{*-}$ ,  $J/\psi\rho$  and  $J/\psi\omega$ . In Fig. 3, we show them for the parameter set A without the meson width. The lines for  $D^0 \bar{D}^{*0}$ ,  $D^+ D^{*-}$ , and  $J/\psi\rho$  correspond to the observed spectrum though the overall factor arising from the weak interaction should be multiplied. In order to obtain the  $J/\psi\pi^3$  spectrum, the fraction  $\tilde{\Gamma}_{\omega \rightarrow 3\pi} = \Gamma_{\omega \rightarrow 3\pi} / \Gamma_{\omega} = 0.892$  [6] should be multiplied furthermore to the  $J/\psi\omega$  spectrum. The spectra are plotted in Fig. (a) for  $3870 \text{ MeV} \leq E \leq 4000 \text{ MeV}$ . In Fig. (b), we plot the same spectra around the  $D^0 \bar{D}^{*0}$  threshold in a different scale. There is a bound  $X(3872)$  at  $3871.68 \text{ MeV}$ , which is marked by a  $\times$  in the Fig. 3 (b). The  $D^+ D^{*-}$  and the  $J/\psi\omega$  spectra are not shown in Fig. (b) because they are still closed. All of the four two-meson channels as well as the  $c\bar{c}$  state are included in the calculations throughout the present article.

As seen from Fig. 3(a), the transfer strength has a peak just above the  $D^0 \bar{D}^{*0}$  threshold. Such a peak appears because the bound state exists very close to the threshold. It, however, is probably difficult to distinguish the strength of this peak from that of the bound state by the experiments of the current resolution. Above the  $D^+ D^{*-}$  threshold, the  $D^0 \bar{D}^{*0}$  and

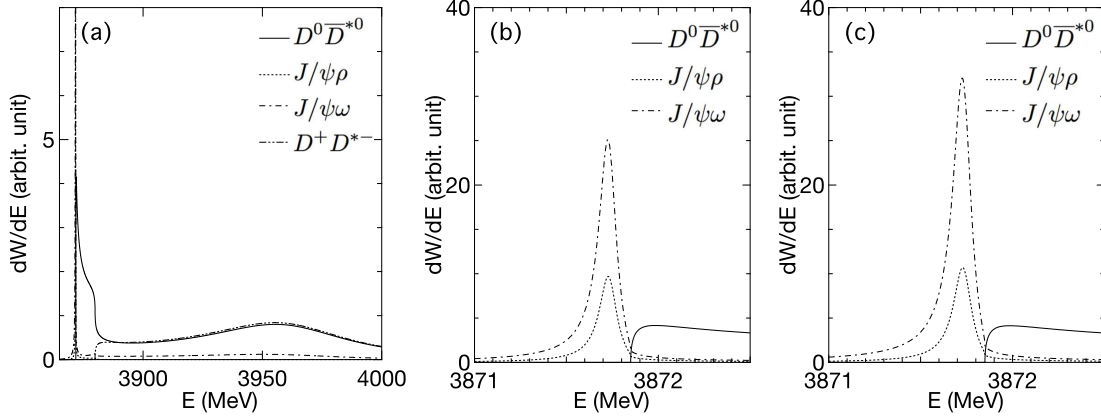


**Fig. 4** The transfer strength from the  $c\bar{c}$  quarkonium to the two-meson states. (a) for  $3870 \text{ MeV} \leq E \leq 4000 \text{ MeV}$  and (b) around the  $D^0 \bar{D}^{*0}$  threshold by the parameter set A with the  $\rho$  and  $\omega$  meson widths. The Fig. (c) corresponds to those by the parameter set A with the energy-independent width.

$D^+ D^{*-}$  spectra are almost the same. The isospin symmetry breaking is restored there, which can also be seen from the fact that the  $J/\psi \rho$  spectrum is almost invisible there. The  $c\bar{c}$  quarkonium mass is 3950 MeV when the  $c\bar{c} - D\bar{D}^*$  coupling is switched off. After the coupling is introduced, the pole moves from 3950 MeV to  $3960 - \frac{i}{2}73 \text{ MeV}$ . All the spectra are found to be rather flat at around 3950 MeV because the imaginary part of the pole energy is large. The pole position in the  $D^0 \bar{D}^{*0}$  channel with the  $c\bar{c}$  state is investigated extensively in ref. [51]. The pole mentioned above corresponds to their ‘confinement pole,’ whereas the bound state corresponds to their ‘dynamical pole.’ The pole position in the present work is similar to that in their work.

The transfer strengths calculated with the  $\rho$  and  $\omega$  meson width are shown in Fig. 4, which correspond again to the parameter set A. The overall feature of the  $D^0 \bar{D}^{*0}$  and  $D^+ D^{*-}$  spectra do not change much when the  $\rho$  and  $\omega$  meson width is introduced. The  $D^0 \bar{D}^{*0}$  peak exists naturally above the threshold. That means the peak energy is higher than that in the  $J/\psi V$  spectrum, which is consistent with the experiment: the  $X(3872)$  mass from  $D^0 \bar{D}^{*0}$  mode =  $3872.9^{+0.6}_{-0.4} {}^{+0.4}_{-0.5}$  for Belle [10], or  $3875.1^{+0.7}_{-0.5} \pm 0.5$  for BABAR [11]. The width of the peak from  $D^0 \bar{D}^{*0}$  mode is found to be a few MeV in our calculation, which is also consistent with the experiments,  $\Gamma_{X \rightarrow D^0 \bar{D}^{*0}} = 3.9^{+2.8}_{-1.4} {}^{+0.2}_{-1.1}$  [10], or  $3.0^{+1.9}_{-1.4} \pm 0.9$  [11]. The  $J/\psi \rho$  and  $J/\psi \omega$  strength around the  $D^0 \bar{D}^{*0}$  threshold, however, change drastically as seen in Fig. 4(b). They make a very thin peak at the  $X(3872)$  mass. Note that the experiments give only an upperbound for the  $X(3872)$  width,  $< 1.2 \text{ MeV}$  in the  $J/\psi \pi^n$  spectrum [7]. The widths of the  $J/\psi V$  peaks here are much smaller than this upperbound. The  $J/\psi \omega$  component appears around the  $D^0 \bar{D}^{*0}$  threshold due to the  $\omega$  decay width though the channel is still

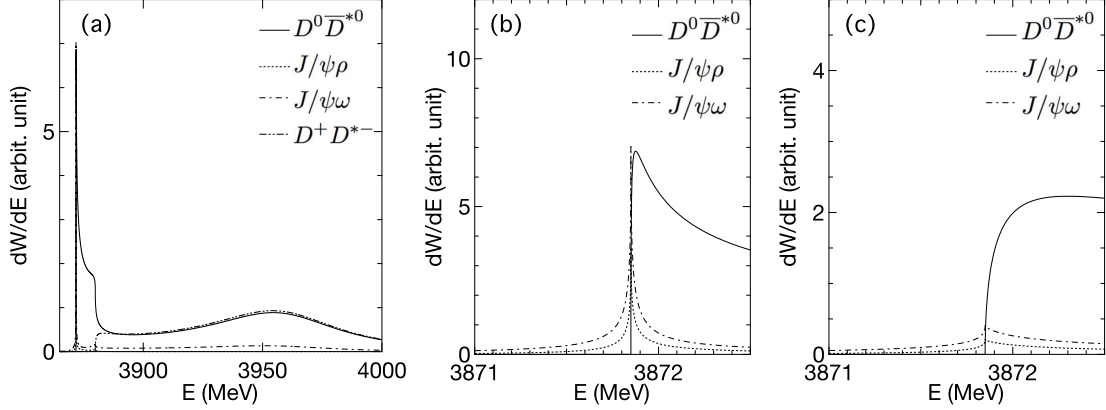


**Fig. 5** The transfer strength from the  $c\bar{c}$  quarkonium to the two-meson states. Parameter set A with the  $\rho$  and  $\omega$  meson widths. The  $c\bar{c}$ - $D\bar{D}^*$  coupling  $g^2$  is weakened by  $0.9g^2$  in Figs. (a) and (b), by  $0.8g^2$  in Fig. (c). Note that the scale of the vertical axis of Fig. (b) or (c) is different from the Figs. 3 or 4.

closed. In the Fig. 4(c), we show the spectrum when the meson widths are taken to be energy independent. The peak reduces when the energy dependent widths are introduced.

To look into the isospin symmetry breaking around the  $D^0\bar{D}^{*0}$  threshold, we calculate ratio of the strength integrated over the range of  $m_X \pm \epsilon_X$ , where  $m_X$  is the average mass of  $X(3872)$ , 3871.68 MeV,  $\epsilon_X$  is the upper bound value of  $\Gamma_{X(3872)}$ , 1.2 MeV.

$$R_\Gamma = \frac{I_{J/\psi\omega}(m_X - \epsilon_X, m_X + \epsilon_X)}{I_{J/\psi\rho}(m_X - \epsilon_X, m_X + \epsilon_X)} \frac{\tilde{\Gamma}_{\omega \rightarrow 3\pi}}{\tilde{\Gamma}_{\rho \rightarrow 2\pi}} \quad (62)$$

$$I_f(E_1, E_2) = \int_{E_1}^{E_2} dE \frac{dW(c\bar{c} \rightarrow f)}{dE} . \quad (63)$$

Here, the factor  $\tilde{\Gamma}_{\omega \rightarrow 3\pi}$  is the fraction of  $\omega \rightarrow \pi\pi\pi$ ,  $0.892 \pm 0.007$ , whereas that of  $\rho$ ,  $\tilde{\Gamma}_{\rho \rightarrow 2\pi}$  is  $\sim 1$  [6]. We assumed the value of the ratio of these fractions to be 0.892. This  $R_\Gamma$  defined above should correspond to the experimental ratio, eqs. (1) and (2),  $1.0 \pm 0.4 \pm 0.3$ [13] or  $0.8 \pm 0.3$ [14]. For the parameter set A, this ratio  $R_\Gamma$  is found to be 2.38, which is somewhat larger than the experiments. There is an estimate by employing a two-meson model, where its value is about 2 [32], whereas in the work of the one-boson exchange model, this value is about 0.3 for a bound state with the binding energy of 0.1 MeV [77]. The present work, having no isospin breaking term in the interaction, gives a closer value to the former case.

As listed in Table 1, the observed  $X(3872)$  mass,  $3871.68 \pm 0.17$  MeV, is very close to the  $D^0\bar{D}^{*0}$  threshold,  $3871.85 \pm 0.20$  MeV. The peak energy of  $X(3872)$  corresponds to the threshold energy within the error bars. There is a possibility that the  $X(3872)$  is not a bound state but a peak at the threshold. In order to see the situation, we also calculate the spectrum by the parameter set A with weakened  $c\bar{c}$ - $D\bar{D}^*$  couplings: the one where the

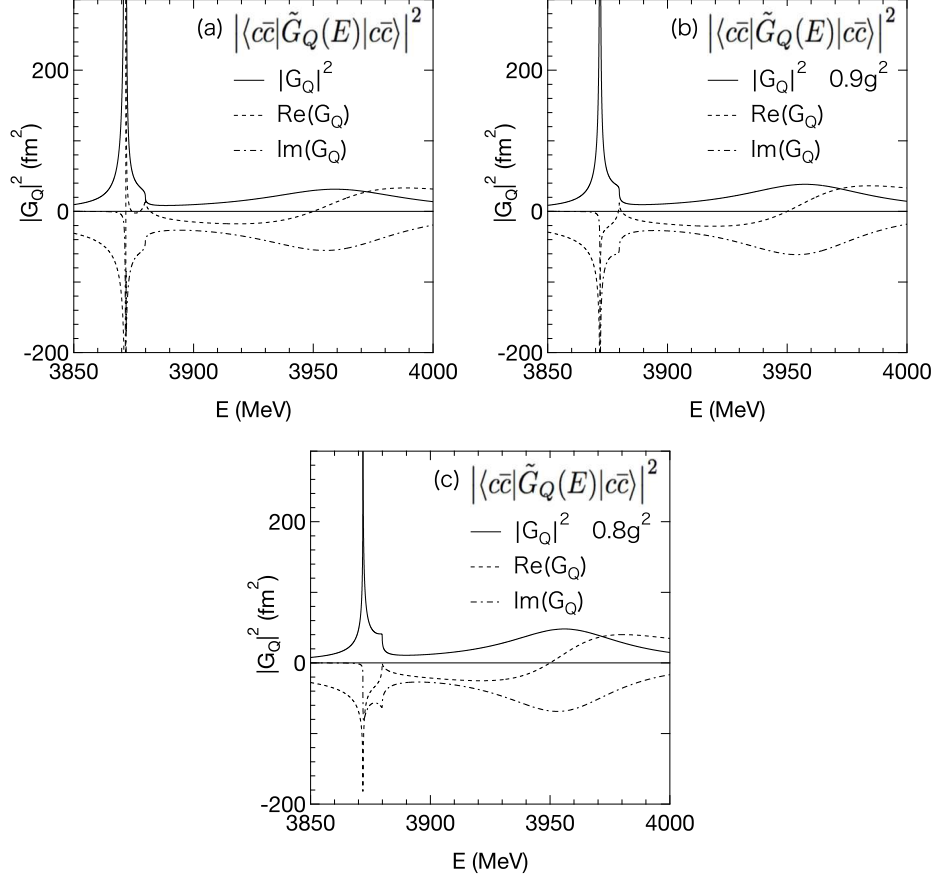


**Fig. 6** Factors of the transfer strength from the  $c\bar{c}$  quarkonium to the two-meson states. (a)  $|\langle c\bar{c}|G_Q(E)|c\bar{c}\rangle|^2$  in eq. (41) for each channel around the  $D^0\bar{D}^{*0}$  threshold for the parameter set A. In Figs. (b) and (c),  $|\langle c\bar{c}|G_Q(E)|c\bar{c}\rangle|^2$  for the  $0.9g^2$  and  $0.8g^2$  cases are shown.

coupling strength  $g^2$  is 0.9 times as large as that of the parameter set A (denoted by  $0.9g^2$  and shown in Figs. 5(a) and (b)) and that of 0.8 (denoted by  $0.8g^2$  and shown in Fig. 5 (c)). There is no bound state anymore but a virtual state in both of the cases, and a peak is still found at the  $D^0\bar{D}^{*0}$  threshold for the  $0.9g^2$  case. The strength of the  $J/\psi V$  channels, however, becomes considerably smaller.

In order to see the mechanism to create a peak at around the threshold and how the peak of each channel is developed, we plot each factor defined by eq. (41) in Figs. 6 and 7. From the Fig. 6, one can see that the full propagator of the  $c\bar{c}$  space,  $G_Q$ , is responsible to make the peak structure. As  $(g/g_0)^2$  is weakened, the bound state becomes a virtual state. But the  $G_Q$  still has a peak at  $0.9g^2$  as seen in Fig. 6(b), which makes a thin peak in the transfer strength. The shape of  $G_Q$  is essentially determined within the  $c\bar{c}$ - $D\bar{D}^*$  system. The effect of the  $J/\psi V$  channel is rather small here.

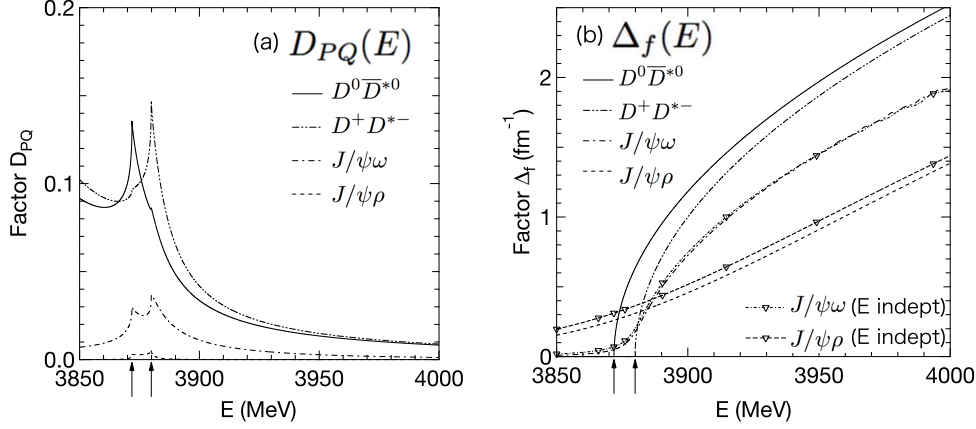


**Fig. 7** Factors of the transfer strength from the  $c\bar{c}$  quarkonium to the two-meson states. (a) the factor  $D_{PQ}$  and (b) the factor  $\Delta_f$  in eq. (41) for each channel around the  $D^0\bar{D}^{*0}$  threshold for the parameter set A. The arrows at the horizontal axis correspond to the  $D^0\bar{D}^{*0}$  and the  $D^+D^{*-}$  threshold energy.

The  $c\bar{c}$  state branches out into each two-meson state by the factor  $D_{PQ}$ . As seen in Fig. 7(a), the factor for the  $J/\psi\rho$  component is very small, while the factor for the  $D^0\bar{D}^{*0}$  and  $D^+D^{*-}$  are comparable to each other. They have a cusp at their threshold. We show  $\Delta_f$  in Fig. 7(b), which is an essentially kinematical factor. Because of the large  $\rho$  meson decay width,  $\Delta_{J/\psi\rho}$  is 5.23 times larger than  $\Delta_{J/\psi\omega}$  at the  $X(3872)$  peak energy. This enhancement factor is smaller than the value given by [43], 13.3. Without this  $\Delta_f$  factor, the branching ratio,  $R_\Gamma$  defined by eq. (62), is about 12.4, due to the large  $D_{PQ}$  for the  $J/\psi\omega$  channel. This value is consistent with the experimentally required value estimated by [58],  $11.5 \pm 5.7$ . Both of  $\Delta_{J/\psi\rho}$  and  $\Delta_{J/\psi\omega}$  become smaller as the energy-dependence of the decay widths are taken into account:  $\Delta_{J/\psi\rho}$  at  $m_{X(3872)}$  reduces from 0.310 to 0.259 while  $\Delta_{J/\psi\omega}$  reduces from 0.069 to 0.049. The ratio of  $\Delta_{J/\psi\omega}$  to  $\Delta_{J/\psi\rho}$  reduces from 0.212 to 0.191; the reduction due to the energy dependence is 0.863. This reduction of  $\Delta_f$  is the reason why the peak with the energy dependent widths is smaller in Fig. 4.

The peak shape is discussed in refs. [42, 48, 50]. The shape of the  $D^0\bar{D}^{*0}$  spectrum around the threshold in these works including ours is essentially the same; The spectrum rises sharply at the threshold, and decreases slowly as the energy increases. As for the  $J/\psi\rho$  or  $J/\psi\omega$  spectrum, it has been reported that a thin peak is produced by employing the resonance expansion [50]. They assume that there is a direct coupling between the  $c\bar{c}$  and  $J/\psi V$  channels. The present model, where the  $J/\psi V$  couples to  $c\bar{c}$  only via  $D\bar{D}^*$  channels, again gives the thin peak. It seems that the model with the quark degrees of freedom with the phenomenological two-meson- $c\bar{c}$  coupling also give a thin peak[48].

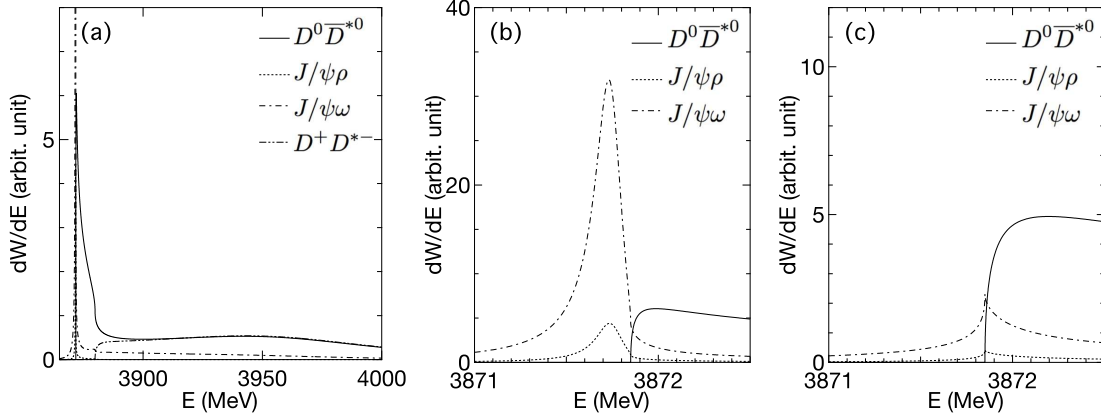


**Fig. 8** The transfer strength from the  $c\bar{c}$  quarkonium to the two-meson states. (a) for  $3870 \text{ MeV} \leq E \leq 4000 \text{ MeV}$  and (b) around the  $D^0\bar{D}^{*0}$  threshold, (c) those with the  $c\bar{c}-D\bar{D}^*$  coupling weakened by  $0.9g^2$ . Parameter set QM.

In the parameter set A, the attraction between the  $D^{(*)}$  and  $\bar{D}^{(*)}$  mesons is taken empirically while the interaction between the  $D\bar{D}^*$  and the  $J/\psi V$  meson channels is taken from the quark model. When we use the quark model value for all the two-meson interaction (parameter set QM), then we have the spectrum shown in Fig. 8. As seen in Table 2, there is no attraction in the  $D\bar{D}^*$  channel, though there is a considerable attraction appears between  $J/\psi$  and the light vector meson. This attraction, however, is not large enough to make a bound state by itself. Most of the attraction to form a bound  $X(3872)$  comes from the  $c\bar{c}-D\bar{D}^*$  coupling; it requires  $(g/g_0)^2 \sim 1$  to have a bound  $X(3872)$ . The  $D\bar{D}^*$  spectrum at around 3950 MeV is very flat, reflecting the fact that the  $c\bar{c}-D\bar{D}^*$  coupling is very strong. There is a large  $J/\psi\omega$  peak at the  $D^0\bar{D}^{*0}$  threshold, while the  $J/\psi\rho$  peak is small. In the case of the weaker coupling,  $0.9g^2$ , (Fig. 8(c)), there is almost no strength in the  $J/\psi\rho$  channel.

To see the parameter dependence, we use a different size of  $v$  or  $u$  in the parameter set B or C, respectively. Their values are 1.5 times larger than those of the parameter set A. The transfer strengths are shown in Figs. 9 and 10. The overall feature of the  $D\bar{D}^*$  channels is similar to that of the parameter set A, though the bump at  $E = 3950 \text{ MeV}$  is enhanced slightly. At the  $D^+D^{*-}$  threshold, a small shoulder appears in the parameter set B. This shoulder develops to an actual peak as the attraction  $v$  becomes stronger. When  $g \sim 0$ , there will be three peaks: if  $v$  is strong enough to have a bound state in  $D^0\bar{D}^{*0}$ , then there will also be a bound state in  $D^+D^{*-}$  provided that the mixing between the  $D^0\bar{D}^{*0}$  and  $D^+D^{*-}$  is small. Moreover, there should be a peak of  $c\bar{c}$ , which couples to  $D\bar{D}^*$  only weakly.

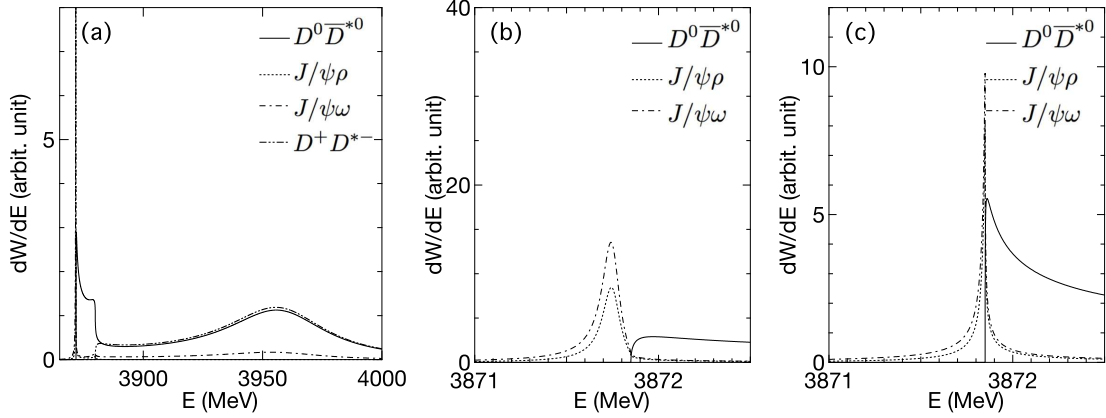


**Fig. 9** The transfer strength from the  $c\bar{c}$  quarkonium to the two-meson states. (a) for  $3870 \text{ MeV} \leq E \leq 4000 \text{ MeV}$  and (b) around the  $D^0 \bar{D}^{*0}$  threshold, (c) those with the  $c\bar{c}-D\bar{D}^*$  coupling weakened by  $0.9g^2$ . Parameter set B.

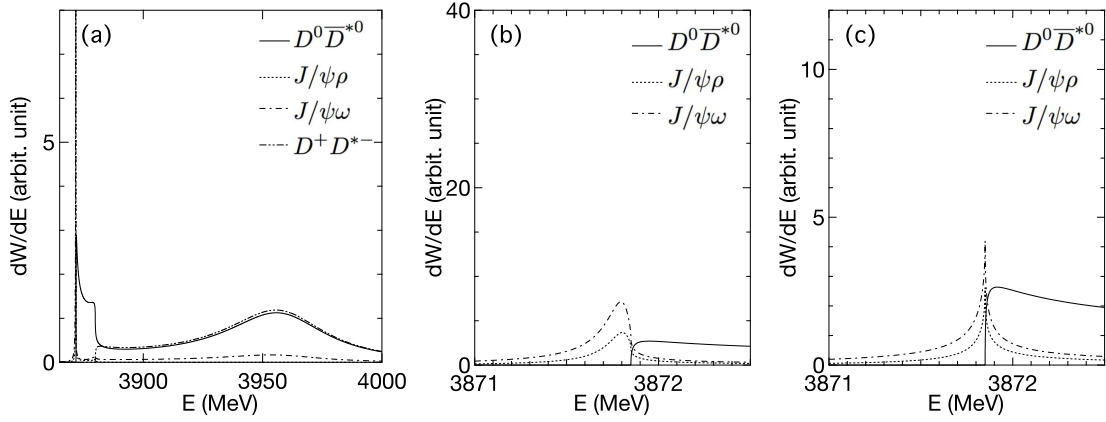


**Fig. 10** The transfer strength from the  $c\bar{c}$  quarkonium to the two-meson states. (a) for  $3870 \text{ MeV} \leq E \leq 4000 \text{ MeV}$  and (b) around the  $D^0 \bar{D}^{*0}$  threshold, (c) those with the  $c\bar{c}-D\bar{D}^*$  coupling weakened by  $0.9g^2$ . Parameter set C.

### 3.3. Various ratios of the transfer strength

In the previous subsection, we show that all of the present parameter sets produce a thin  $J/\psi\pi^n$  peak at around the  $D^0 \bar{D}^{*0}$  threshold. The mechanism to form  $X(3872)$ , however, is different from each other. To look into what kinds of observables can be used to distinguish the models, we listed the values of various ratios of the transfer strength in Table 6.

It is found that the values of the ratio  $R_\Gamma$  defined by Eq. (62) vary rather widely according to the parameters. As the  $(g/g_0)^2$  becomes smaller, the ratio  $R_\Gamma$  becomes smaller, and the degree of the isospin symmetry breaking becomes larger. The binding energy of  $X(3872)$ , or the effect of the energy dependence of the  $\rho$  and  $\omega$  meson width seems to be rather

**Table 6** Various ratios of the transfer strength for the original parameter set A, B, C, and QM, and those with the weakened  $c\bar{c}-D\bar{D}^*$  coupling, which are denoted by  $0.9g^2$ .  $A_0$  is the parameter set A with the energy-independent meson width. As for the definition of the ratios, see text. The Belle experiment of  $R_\Gamma$  is taken from ref. [13], while that of *BABAR* is taken from ref. [14]. As for the  $r_{D^0\bar{D}^{*0}}$ , the Belle value is taken from refs. [7, 10] while that of *BABAR* is taken from refs. [11, 12].

Model	$(g/g_0)^2$	$R_\Gamma$	$r_{D^0\bar{D}^{*0}}(4\text{MeV})$	$r_{D^0\bar{D}^{*0}}(8\text{MeV})$	$D_{I=1/0}$
A	0.66	2.38	5.56	8.40	0.0839
A( $0.9g^2$ )	0.59	2.04	20.11	25.96	0.0879
$A_0$	0.66	2.76	4.82	7.26	0.0834
$A_0(0.9g^2)$	0.59	2.36	16.88	21.84	0.0872
B	0.48	1.48	4.34	6.73	0.0463
B( $0.9g^2$ )	0.43	1.29	10.23	13.89	0.0447
C	0.50	1.92	4.77	6.69	0.0529
C( $0.9g^2$ )	0.45	1.77	8.11	10.42	0.0487
QM	1.00	6.67	10.96	15.26	0.1425
QM( $0.9g^2$ )	0.90	5.86	41.49	51.17	0.1526
Belle		$1.0 \pm 0.4 \pm 0.3$		$8.92 \pm 2.42$	
<i>BABAR</i>		$0.8 \pm 0.3$		$19.9 \pm 8.05$	

small here. The situation is illustrated in Fig. 11 (a). The parameter QM, where  $(g/g_0)^2$  is about 1, the ratio  $R_\Gamma$  is 6.67. For the parameter set A, where  $(g/g_0)^2 = 0.66$ , the value is 2.38. For the parameter sets B or C, the value becomes around  $1.29 \sim 1.92$ . The  $R_\Gamma$  is defined by integrating the strength over  $m_X \pm 1.2$  MeV. The values of  $R_\Gamma$  do not change much if we integrate the strength over  $m_X \pm 2.4$  MeV; the largest deviation is less than 3% of the listed value. Though the values we obtained here are still larger than the observed ones, they agree with the experiment qualitatively. The experimental results suggest that  $(g/g_0)^2 \sim 0.3 \sim 0.5$ . The relative importance of the  $c\bar{c}-D\bar{D}^*$  coupling,  $(g/g_0)^2$ , together with the factor  $\Delta_f$ , surely play important roles in the mechanism to have the isospin symmetry breaking of this size. Oppositely, one can estimate the sizes of the  $c\bar{c}-D\bar{D}^*$  coupling as well as the attraction between  $D$  and  $\bar{D}^*$  from the observed size of the isospin symmetry breaking.

In Fig. 11 (b) and Table 6, we also show the ratio between the  $D^0\bar{D}^{*0}$  and  $D^+D^{*-}$  strengths:

$$D_{I=1/0} = \frac{I_{D^0\bar{D}^{*0}}(m_{D^0} + m_{\bar{D}^{*0}}, \infty) - I_{D^+D^{*-}}(m_{D^+} + m_{D^{*-}}, \infty)}{I_{D^0\bar{D}^{*0}}(m_{D^0} + m_{\bar{D}^{*0}}, \infty) + I_{D^+D^{*-}}(m_{D^+} + m_{D^{*-}}, \infty)}. \quad (64)$$

This  $D_{I=1/0}$  essentially describes the ratio of the  $D\bar{D}^*$  strength below and above the  $D^+D^{*-}$  threshold, which is found to be governed by the relative importance of the  $c\bar{c}-D\bar{D}^*$  coupling against the  $D-\bar{D}^*$  attraction,  $(g/g_0)^2$ . No experimental result has been reported for this value, but with this and the size of the isospin symmetry breaking, the information on the

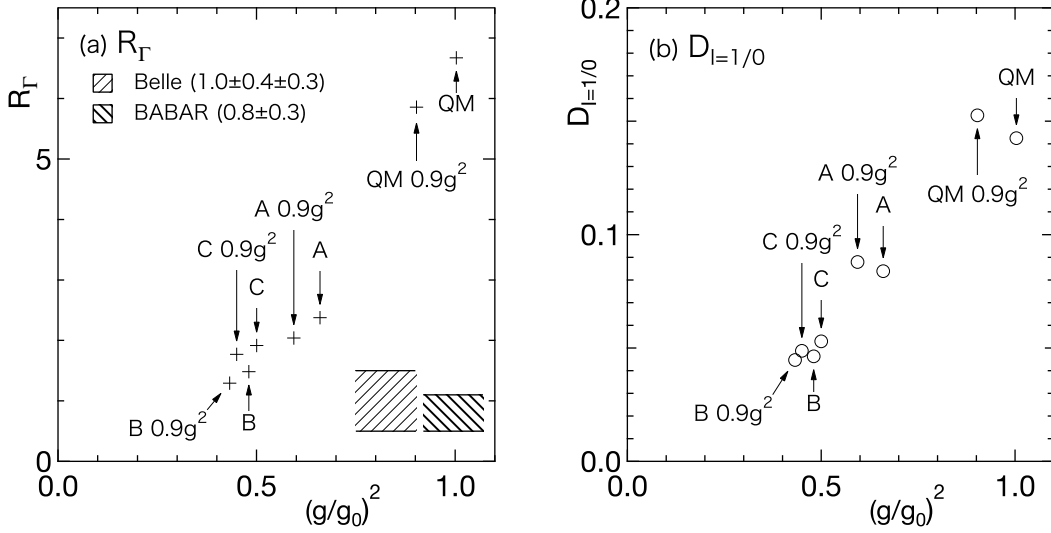


**Fig. 11** The  $J/\psi\pi^3$ - $J/\psi\pi^2$  ratio at the  $X(3872)$  peak,  $R_\Gamma$ , and the  $D^0\bar{D}^{*0}$ - $D^+D^{*-}$  ratio integrated over the scattering state,  $D_{I=1/0}$ . In the Fig. (a), the  $R_\Gamma$  is plotted against  $(g/g_0)^2$ , while  $D_{I=1/0}$  is plotted in Fig. (b). The experimental results for  $R_\Gamma$  [13, 14], which do not depend on the  $(g/g_0)^2$ , are shown in Fig. (a) by the hatched areas.

$X(3872)$  structure, or on the size of the the  $c\bar{c}$ - $D\bar{D}^*$  coupling or the heavy meson interaction will become much clearer.

The ratio  $r_{D^0\bar{D}^{*0}}$  is defined as

$$r_{D^0\bar{D}^{*0}} = \frac{I_{D^0\bar{D}^{*0}}(m_{X(3872)} - \epsilon, m_{X(3872)} + \epsilon)}{I_{J/\psi\rho}(m_{X(3872)} - \epsilon, m_{X(3872)} + \epsilon)}. \quad (65)$$

We listed  $r_{D^0\bar{D}^{*0}}$  for  $\epsilon = 4$  MeV and 8 MeV in Table 6. It is found that for the parameter sets which are  $(g/g_0)^2 \sim 0.5$ , this  $r_{D^0\bar{D}^{*0}}$  is about 4.34-8.40 if the  $X(3872)$  is a bound state, while the value is more than 8 if there is no bound state, as the ones denoted by  $0.9g^2$ . As we mentioned in the introduction, the experiments for this ratio is still controversial. More precise measurements will help to determine whether the  $X(3872)$  is a bound state or not.

In the present calculation, the range is  $\Lambda = 500$  MeV for all the interaction because we use a simple model with the separable approximation. The attraction between the  $D$  and  $\bar{D}^*$  mesons, however, is considered to come from the  $\pi$ - and  $\sigma$ -meson exchange, which has much longer range than that of the  $D\bar{D}^*$ - $J/\psi V$  or  $c\bar{c}$ - $D\bar{D}^*$  coupling. We neglect the coupling between the orbital  $S$ - and  $D$ -wave. The present results may change quantitatively if one introduces more realistic interaction. We expect, however, that the mechanism to have a thin peak or to enhance the  $I = 1$  component will not change. Let us mention that our results do not exclude that the existence of other sources of the isospin symmetry breaking, which contribute to reduce the ratio  $R_\Gamma$ . It will be interesting to see how the combined effects change the ratio.

---

Since the mass of the  $\chi_b$  meson is not nearby  $B\bar{B}^*$  threshold, the  $I = 0$   $B\bar{B}^*$  system does not have the extra attraction from the  $b\bar{b}$ - $B\bar{B}^*$  coupling like the  $D\bar{D}^*$  systems. Namely the most important interaction in the  $B\bar{B}^*$  system will be the interaction between the  $B$  and  $\bar{B}^*$  mesons. If the interaction between the  $D$  and  $\bar{D}^*$  mesons in the present work is applied to the  $B\bar{B}^*$  system as it is, there will be a zero-energy resonance for the parameter set A or C. As for the parameter set B, a bound state whose binding energy is 2.4 MeV appears. It will be very interesting and contributing to understand the heavy quark physics if one finds out whether such a bound state exists in the  $B\bar{B}^*$  systems. In the  $B^{(*)}\bar{B}^*$  systems, the situation of the  $I = 0$  and 1 channels is similar in the sense that there is no core- $B^{(*)}\bar{B}^*$  coupling which gives an extra attraction. The interaction between the  $B$  and  $\bar{B}^*$  mesons is considered to determine the bulk features of the systems. Experimentally, no bound state has been found yet but for the  $Z_b(10610)^{\pm,0}$  and the  $Z_b(10650)^{\pm}$  resonances. Though they are not considered as simple  $S$ -wave resonances, it is very likely that the attraction between the  $B$  and the  $\bar{B}^*$  mesons to make such peaks is comparable in size with that which gives a zero-energy resonance. The potential we assumed for  $D\bar{D}^*$  system is consistent with these experimentally observed properties of the  $B^{(*)}\bar{B}^*$  systems.

#### 4. Summary

The  $X(3872)$  and the two-meson spectrum from the  $B$ -decay are investigated by a  $c\bar{c}$ -two-meson hybrid model for the energy from around the  $D^0\bar{D}^{*0}$  threshold up to 4 GeV. The two-meson state consists of the  $D^0\bar{D}^{*0}$ ,  $D^+D^{*-}$ ,  $J/\psi\rho$ , and  $J/\psi\omega$ . The final states are investigated separately for each channel. The energy dependent decay widths of the  $\rho$  and  $\omega$  mesons are taken into account. The coupling between the  $D\bar{D}^*$  and the  $J/\psi V$  channels is determined from the quark model. The attraction between the  $D$  and  $\bar{D}^*$  is determined so that it produces a zero-energy resonance but no bound state if the attraction of the same size is introduced in the  $B\bar{B}^*$  system. The strength of the  $c\bar{c}$ - $D\bar{D}^*$  coupling is taken to be a free parameter to give the correct  $X(3872)$  mass.

We have found that the  $X(3872)$  can be a shallowly bound state or a  $S$ -wave virtual state. For both of the cases, the following two notable features are found: (1) both of the  $c\bar{c} \rightarrow J/\psi\rho$  and  $c\bar{c} \rightarrow J/\psi\omega$  mass spectra have a very narrow peak below or on the  $D^0\bar{D}^{*0}$  threshold, and (2) the strength of the  $J/\psi\pi^2$  peak is comparable to that of the  $J/\psi\pi^3$  peak.

The feature (1) implies that the observed peak found in the  $J/\psi\pi^n$  spectrum may not directly correspond to the pole energy of the  $X(3872)$ . It may be a peak at the threshold caused by a virtual state. If the  $X(3872)$  is a bound state, then the peak which corresponds to the pole energy appears below the  $D^0\bar{D}^{*0}$  threshold. The current experiments cannot distinguish these two cases. As for the feature (2), the present work shows that the isospin symmetry breaking caused by the neutral and charged  $D^{(*)}$  meson mass difference seems to

be large enough to explain the experiments owing to the enhancement by the large  $\rho$  meson width. When the peak strength is integrated over the interval  $E = m_{X(3872)} \pm 1.2$  MeV, the decay ratio,  $R_\Gamma$ , becomes 1.29-2.38. Though this is still larger than the observed values,  $1.0 \pm 0.4 \pm 0.3$  or  $0.8 \pm 0.3$ , the obtained values agree with the experiment qualitatively.

The size of the isospin symmetry breaking in the transfer strength becomes larger as the  $c\bar{c}-D\bar{D}^*$  coupling becomes weaker. The relative strength of the  $D^0\bar{D}^{*0}$  below the  $D^+D^{*-}$  threshold also varies largely according to the size of this coupling. We would like to point out that from these two observables combined, the information on the size of the  $c\bar{c}-D\bar{D}^*$  coupling or the heavy meson interaction can be obtained more clearly. It is also found that the branching ratio of the  $D^0\bar{D}^{*0}$  to the  $J/\psi\rho$ , which is still controversial experimentally, is a good indicator of evaluating whether the  $X(3872)$  peak is a bound state or a virtual state. Investigating the  $X(3872)$  properties really gives us rich information on the heavy quark physics.

## A. Appendix: Width of the $\rho$ and $\omega$ mesons

### A.1. Kinematics

The  $B^+$  meson at rest has the mass  $m_B = 5279.26 \pm 0.17$  MeV [6]. It can decay into  $K^+$  and a  $c\bar{c}$  pair by the weak interaction. When this  $K$  meson has the momentum  $\mathbf{p}_K$ , then the  $X(3872)$ , which is generated from the  $c\bar{c}$  pair, has the energy  $E_X$  as

$$E_X = m_B - \sqrt{m_K^2 + p_K^2} \quad (\text{A1})$$

with the momentum  $\mathbf{p}_X = -\mathbf{p}_K$ .

Suppose the  $X(3872)$  is a bound state and does not decay, it has the center of mass momentum  $\mathbf{p}_X$  and the energy  $E_X = \sqrt{m_{X(3872)}^2 + p_X^2}$ . Thus the size of  $\mathbf{p}_K$  is uniquely determined once  $m_{X(3872)}$  is given: *e.g.* when  $m_{X(3872)} = 3871.68$  MeV,  $p_K = 5.78$  fm $^{-1}$ .

On the other hand, suppose the  $X(3872)$  is a resonance and the final states are the scattering two mesons, the phase space of the kaon momentum  $\mathbf{p}_K$  becomes a continuum. The energy of the two mesons in the  $f$ -th channel, whose center of mass momentum is  $\mathbf{p}_X = -\mathbf{p}_K$ , can be written as

$$E_X = \sqrt{(M_f + m_f)^2 + p_X^2} + \frac{k_f^2}{2\mu_f}, \quad (\text{A2})$$

where  $m_f$  and  $M_f$  are each of the masses of the final two mesons, the  $\mu_f$  their reduced mass, and  $\mathbf{k}_f$  the relative momentum of the two mesons. Here we extract the relative motion in a nonrelativistic way. Since we investigate the reaction only slightly above the threshold,  $k_f$  is considered to be small comparing to the meson masses.

The energy of the two-meson system at rest,  $E_f$ , can be defined as

$$E_f = M_f + m_f + \frac{k_f^2}{2\mu_f} \quad (\text{A3})$$

$$= M_f + m_f + E_X - \sqrt{(M_f + m_f)^2 + p_X^2}. \quad (\text{A4})$$

The figures in this paper are plotted against this energy  $E_f$  for the  $D^0\bar{D}^{*0}$  channel,  $E_{D^0\bar{D}^{*0}}$ .

When the final two mesons are  $J/\psi$  and  $\rho$ , for example, the above  $E_f$  becomes

$$E_{J/\psi\rho} = m_{J/\psi} + m_\rho + \frac{k_{J/\psi\rho}^2}{2\mu_{J/\psi\rho}}, \quad (\text{A5})$$

where  $k_{J/\psi\rho}$  is the relative momentum of  $J/\psi$  and  $\rho$  when the  $J/\psi\rho$  system is at rest.

For a given  $|\mathbf{p}_X| (= |\mathbf{p}_K|)$ ,  $E_X$  is determined by Eq. (A1). Then the momentum  $k_{J/\psi\rho}$  is obtained by Eq. (A2), and  $E_{J/\psi\rho}$  by Eq. (A3).

When the  $\rho$  meson decays into the two-pion state, that  $E_{J/\psi\rho}$  can be expressed also by

$$E_{J/\psi\rho} = \sqrt{m_{J/\psi}^2 + k^2} + \sqrt{(2m_\pi)^2 + k^2} - 2m_\pi + E_{2\pi} \quad (\text{A6})$$

$$E_{2\pi} = 2\sqrt{m_\pi^2 + q^2} \quad \text{or} \quad q^2 = \frac{1}{4}E_{2\pi}^2 - m_\pi^2. \quad (\text{A7})$$

Here,  $k$  is the relative momentum between  $J/\psi$  and the center of mass motion of the two pions. The relative momentum between the two pions is denoted as  $q$ , and  $E_{2\pi}$  is the energy of the two pions whose center of mass motion is zero. The energy  $E_{2\pi}$  becomes a function of  $k$  and  $k_{J/\psi\rho}$ ,  $E_{2\pi}(k, k_{J/\psi\rho})$ . Note that  $k$  can be different from  $k_{J/\psi\rho}$ ;  $k_{J/\psi\rho}$  and  $k$  correspond to  $k_f$  and  $k$  in Eq. (39) respectively.

When the final two mesons are  $J/\psi$  and  $\omega$ , which decays into the three-pion state, the center of mass energy of the  $J/\psi$  and  $\omega$  system,  $E_{J/\psi\omega}$  can be rewritten similarly by

$$E_{J/\psi\omega} = \sqrt{m_{J/\psi}^2 + k^2} + \sqrt{(3m_\pi)^2 + k^2} - 3m_\pi + E_{3\pi}, \quad (\text{A8})$$

where  $E_{3\pi}$  is the energy of the three pions whose center of mass momentum equals to zero. Again, the energy  $E_{3\pi}$  becomes a function of  $k$  and  $k_{J/\psi\omega}$ ,  $E_{3\pi}(k, k_{J/\psi\omega})$ . For the later convenience, we define the ‘average’ momentum,  $\bar{q}$ , as

$$\bar{q}^2 = \frac{1}{9}E_{3\pi}^2 - m_\pi^2. \quad (\text{A9})$$

## A.2. The $\rho$ and $\omega$ meson width

In this appendix, we show how we obtain the energy dependence of the  $\rho$  and  $\omega$  meson width. Since our main interest is on the X(3872), we only consider the major decay mode for both of the  $\rho$  and  $\omega$  mesons [6]. By assuming that the non-resonant term is small, the cross section,  $\sigma$ , of the mesons can be written as

$$\sigma(E_{n\pi}) \propto \frac{12\pi}{q^2} \frac{\frac{1}{4}\Gamma_V(E_{n\pi})^2}{(E_{n\pi} - \tilde{m}_V)^2 + \frac{1}{4}\Gamma_V(E_{n\pi})^2}, \quad (\text{A10})$$

Here  $\tilde{m}_V$  and  $\Gamma_V(E_{n\pi})$  are the mass and the width of the  $\rho$  and  $\omega$  mesons, respectively, and  $q$  stands for the relative momentum of the two pions which decay from the  $\rho$  meson, Eq. (A7), or for the average momentum of three pions from the  $\omega$  meson, Eq. (A9).

The major decay mode of the  $\rho$  meson is  $\rho \rightarrow \pi\pi$  ( $P$ -wave). The width has a large energy dependence. We rewrite the width as:

$$\Gamma_\rho(E_{2\pi}) = \Gamma_\rho^{(0)} \frac{F_\rho(E_{2\pi})}{F_\rho(\tilde{m}_\rho)}. \quad (\text{A11})$$

Here  $\Gamma_\rho^{(0)}$  is a constant and corresponds to the  $\rho$  meson width at  $E = \tilde{m}_\rho$ , for which we use the observed value. We assume the following function form for  $F_\rho(E_{2\pi})$ .

$$F_\rho(E_{2\pi}) = q^3 \left( \frac{\Lambda_V^2}{\Lambda_V^2 + q^2} \right)^2, \quad (\text{A12})$$

**Table A1** Parameters for the  $\rho$  and  $\omega$  meson width. The values for  $\Gamma_\rho^{(0)}$ ,  $m_\omega$ , and  $\Gamma_\omega^{(0)}$  are the observed ones. All entries are in MeV.

$\tilde{m}_\rho$	$\Gamma_\rho^{(0)}$	$m_\omega$	$\Gamma_\omega^{(0)}$	$\Lambda_V$
768.87	149.1	782.65	8.49	291.05

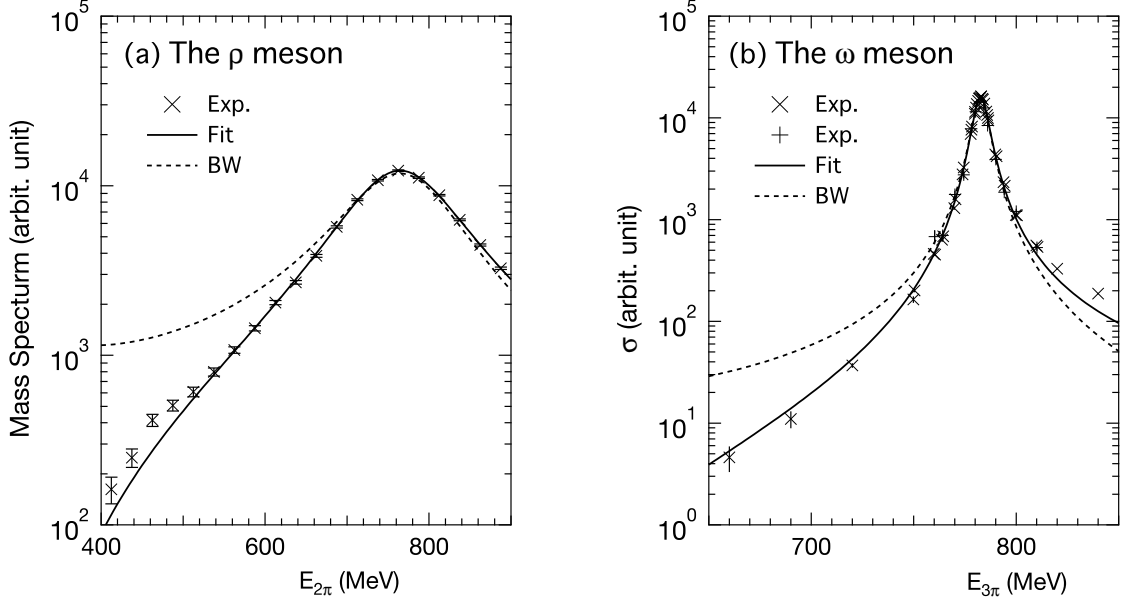


**Fig. A1** The  $\rho$  and  $\omega$  meson decay: (a) the mass spectrum  $\tau^- \rightarrow \pi^- \pi^0 \nu_\tau$  decay, where the data are taken from ref. [91] and (b) the  $e^+e^- \rightarrow \pi^+ \pi^- \pi^0$  cross section where data are taken from ref. [93, 94]. The solid lines are fitted results by employing the energy-dependent width,  $\Gamma_V(E)$ , while dotted lines (BW) are obtained with a energy-independent width,  $\Gamma_V^{(0)}$ .

where  $q^2 = \frac{1}{4}E_{2\pi}^2 - m_\pi^2$  is the relative momentum of the pions and  $\Lambda_V$  is a momentum cutoff. This corresponds to the one with the monopole form factor for relative  $P$ -wave pions.

In Fig. A1(a), the mass spectrum of the  $\rho$  meson,  $\sigma q$ , is plotted against  $E_{2\pi}$ . The experimental data taken from ref. [91] are shown with the error bars. The solid line is the one we calculated with the energy dependent width, where we use the values of  $\tilde{m}_\rho$  and  $\Lambda_V$  as well as the absolute size of the spectrum as fitting parameters. They are shown in Table A1 with the observed width  $\Gamma_\rho^{(0)}$ . The dotted line corresponds to the one without energy dependence,  $\Gamma_\rho = \Gamma_\rho^{(0)}$ .

When we apply the width to the  $X(3872)$ , the factor  $\Delta_f(E)$  appears as seen in Eq. (42). For the energy around the  $D^0 \bar{D}^{*0}$  threshold, this factor for the  $J/\psi$ - $\rho$  channel is sizable only at around  $0 < k \lesssim 3 \text{ fm}^{-1}$ , and takes a maximum value at  $k \sim 1.26 \text{ fm}^{-1}$ . This corresponds to  $E_{2\pi} = 340 \sim 775 \text{ MeV}$  with the maximum at around 670 MeV. Thus we fit rather lower energy region of the  $\rho$  meson peak, 400-900 MeV, to obtain the energy dependent  $\rho$ -meson width.

The  $\omega$  meson decays occurs mainly via a  $\rho\pi$  state (Gell-Mann Sharp Wagner (GSW) mode[92]) at around the peak energy. Also for the  $\omega$  meson we rewrite the width as

$$\Gamma_\omega(E) = \Gamma_\omega^{(0)} \frac{F_\omega(E)}{F_\omega(m_\omega)}, \quad (\text{A13})$$

where  $\Gamma_\omega^{(0)}$  is a constant and corresponds to the  $\omega$  meson width at  $E = m_\omega$ , which we use again the observed total decay width of  $\omega$ . We use a simple form for the energy dependence also for the  $\omega$  meson,

$$F_\omega(E) = \bar{q}^6 \left( \frac{\Lambda_V^2}{\Lambda_V^2 + \bar{q}^2} \right)^4. \quad (\text{A14})$$

where  $\bar{q}^2 = \frac{1}{9}E^2 - m_\pi^2$ . Here we use the same value for the momentum cut-off  $\Lambda_V$  as that we obtained for the  $\rho$  meson. This shape of the energy dependence can be derived by assuming the  $\rho\pi$   $P$ -wave decay has also the monopole form factor, and the energy dependence of the imaginary part of the  $\rho$  meson propagator is governed by that of the  $\rho$  meson form factor. Here we do not discuss whether this assumption is appropriate. We employ the above function form because it is simple and the fitting is good enough to perform our  $X(3872)$  calculation.

In Fig. A1(b), the cross sections of  $\omega$  meson are shown. The data are taken from [93, 94]. The solid line stands for the one with the energy dependent width, and the dotted one is the one without the energy dependence. For the  $\omega$  meson, the factor  $\Delta_f(E)$  in Eq. (42) has a sizable value at around  $0 < k \lesssim 2 \text{ fm}^{-1}$ , and takes a maximum value at  $k \sim 0.5 \text{ fm}^{-1}$ . This corresponds to  $E_{3\pi} = 600 \sim 775 \text{ MeV}$  with the maximum at  $762 \text{ MeV}$ . We fit the data in the energy region  $660\text{-}786 \text{ MeV}$  for the  $\omega$  meson peak.

For both of the  $\rho$  and  $\omega$  decay, we can fit the data with an enough accuracy for the current purpose. The values of parameters are summarized in Table A1. We use only the fitting parameter  $\Lambda_V$  (and function forms of the energy dependence,  $F_\rho$  and  $F_\omega$ ) for the  $X(3872)$  calculation.

## B. Appendix: Meson Interaction obtained from a quark model

### B.1. Base of the two-meson wave functions

The color-spin-flavor part of the wave function for the  $J^{PC} = 1^{++}$   $q\bar{q}c\bar{c}$  state has two components, which may be written by the color singlet and octet  $J/\psi$  with the light vector meson:

$$|V_1 J/\psi_1\rangle = \left[ |q\bar{q} \ S=1, \text{ color } 1\rangle \otimes |c\bar{c} \ S=1, \text{ color } 1\rangle \right]_{\text{color } 1} \quad (\text{B1})$$

$$|V_8 J/\psi_8\rangle = \left[ |q\bar{q} \ S=1, \text{ color } 8\rangle \otimes |c\bar{c} \ S=1, \text{ color } 8\rangle \right]_{\text{color } 1}, \quad (\text{B2})$$

where  $V = \omega$  or  $\rho$ ,  $q$  stands for one of the light quarks,  $u$  and  $d$ ,  $S$  is the spin of the two quarks or the two antiquarks, and color 1 [color 8] stands for the color singlet [octet] state.

These components can be expressed by rearranged ones, such as

$$\begin{aligned} |\bar{D}_1 D^*_1\rangle &= \frac{1}{\sqrt{2}} \left( \left[ |q\bar{c} \ S=0, \text{ color } 1\rangle \otimes |c\bar{q} \ S=1, \text{ color } 1\rangle \right]_{\text{color } 1} \right. \\ &\quad \left. - \left[ |q\bar{c} \ S=1, \text{ color } 1\rangle \otimes |c\bar{q} \ S=0, \text{ color } 1\rangle \right]_{\text{color } 1} \right) \end{aligned} \quad (\text{B3})$$

$$\begin{aligned} |\bar{D}_8 D^*_8\rangle &= \frac{1}{\sqrt{2}} \left( \left[ |c\bar{c} \ S=0, \text{ color } 8\rangle \otimes |q\bar{q} \ S=1, \text{ color } 8\rangle \right]_{\text{color } 1} \right. \\ &\quad \left. - \left[ |c\bar{c} \ S=1, \text{ color } 8\rangle \otimes |q\bar{q} \ S=0, \text{ color } 8\rangle \right]_{\text{color } 1} \right). \end{aligned} \quad (\text{B4})$$

These two color-spin-flavor base functions can be transferred from each other as:

$$\begin{pmatrix} |\bar{D}_1 D^*_1\rangle \\ |\bar{D}_8 D^*_8\rangle \end{pmatrix} = \begin{pmatrix} \sqrt{\frac{1}{9}} & \sqrt{\frac{8}{9}} \\ \sqrt{\frac{8}{9}} & -\sqrt{\frac{1}{9}} \end{pmatrix} \begin{pmatrix} |V_1 J/\psi_1\rangle \\ |V_8 J/\psi_8\rangle \end{pmatrix}. \quad (\text{B5})$$

When one considers the hadronic system, the color-spin-flavor base will be  $|\bar{D}_1 D^*_1\rangle$  and  $|V_1 J/\psi_1\rangle$ , which are not orthogonal to each other from the quark model viewpoint, especially at the short distance. The normalization in the color-spin-flavor space becomes

$$N = \begin{pmatrix} 1 & \frac{1}{3} \\ \frac{1}{3} & 1 \end{pmatrix}. \quad (\text{B6})$$

## Acknowledgement

This work is partly supported by Grants-in-Aid for scientific research (20540281 and 21105006).

## References

- [1] S. K. Choi *et al.* [Belle Collaboration], Phys. Rev. Lett. **91**, 262001 (2003).
- [2] D. Acosta *et al.* [CDF Collaboration], Phys. Rev. Lett. **93**, 072001 (2004).
- [3] V. M. Abazov *et al.* [D0 Collaboration], Phys. Rev. Lett. **93**, 162002 (2004).
- [4] B. Aubert *et al.* [BaBar Collaboration], Phys. Rev. D **71**, 071103 (2005).
- [5] R. Aaij *et al.* [LHCb Collaboration], Eur. Phys. J. C **72**, 1972 (2012).
- [6] J. Beringer *et al.* [Particle Data Group Collaboration], Phys. Rev. D **86**, 010001 (2012).
- [7] S. -K. Choi, S. L. Olsen, K. Trabelsi, I. Adachi, H. Aihara, K. Arinstein, D. M. Asner and T. Aushev *et al.*, Phys. Rev. D **84**, 052004 (2011).
- [8] A. Abulencia *et al.* [CDF Collaboration], Phys. Rev. Lett. **98**, 132002 (2007).
- [9] R. Aaij *et al.* [LHCb Collaboration], Phys. Rev. Lett. **110**, no. 22, 222001 (2013).
- [10] T. Aushev *et al.* [Belle Collaboration], Phys. Rev. D **81**, 031103 (2010).
- [11] B. Aubert *et al.* [BaBar Collaboration], Phys. Rev. D **77**, 011102 (2008).
- [12] B. Aubert *et al.* [BaBar Collaboration], Phys. Rev. D **77**, 111101 (2008).
- [13] K. Abe *et al.* [Belle Collaboration], arXiv:hep-ex/0505037.
- [14] P. del Amo Sanchez *et al.* [BaBar Collaboration], Phys. Rev. D **82**, 011101 (2010).
- [15] T. -W. Chiu *et al.* [TWQCD Collaboration], Phys. Lett. B **646**, 95 (2007).
- [16] S. Prelovsek and L. Leskovec, Phys. Rev. Lett. **111**, 192001 (2013).
- [17] F. E. Close and P. R. Page, Phys. Lett. B **578**, 119 (2004).
- [18] M. B. Voloshin, Phys. Lett. B **579**, 316 (2004).
- [19] C. -Y. Wong, Phys. Rev. C **69**, 055202 (2004).
- [20] E. S. Swanson, Phys. Lett. B **588**, 189 (2004).
- [21] N. A. Tornqvist, Phys. Lett. B **590**, 209 (2004).
- [22] E. S. Swanson, Phys. Lett. B **598**, 197 (2004).
- [23] M. B. Voloshin, Phys. Lett. B **604**, 69 (2004).
- [24] M. T. AlFiky, F. Gabbiani and A. A. Petrov, Phys. Lett. B **640**, 238 (2006).
- [25] S. Fleming, M. Kusunoki, T. Mehen and U. van Kolck, Phys. Rev. D **76**, 034006 (2007).
- [26] E. Braaten and M. Lu, Phys. Rev. D **76**, 094028 (2007).

- 
- [27] E. Braaten and M. Lu, Phys. Rev. D **77**, 014029 (2008).
  - [28] Y. -R. Liu, X. Liu, W. -Z. Deng and S. -L. Zhu, Eur. Phys. J. C **56**, 63 (2008).
  - [29] D. L. Canham, H. -W. Hammer and R. P. Springer, Phys. Rev. D **80**, 014009 (2009).
  - [30] E. Braaten and J. Stapleton, Phys. Rev. D **81**, 014019 (2010).
  - [31] I. W. Lee, A. Faessler, T. Gutsche and V. E. Lyubovitskij, Phys. Rev. D **80**, 094005 (2009).
  - [32] D. Gamermann, J. Nieves, E. Oset and E. Ruiz Arriola, Phys. Rev. D **81**, 014029 (2010).
  - [33] P. Wang and X. G. Wang, Phys. Rev. Lett. **111**, no. 4, 042002 (2013).
  - [34] T. Barnes and S. Godfrey, Phys. Rev. D **69**, 054008 (2004).
  - [35] T. Barnes, S. Godfrey and E. S. Swanson, Phys. Rev. D **72**, 054026 (2005).
  - [36] M. Butenschoen, Z. -G. He and B. A. Kniehl, Phys. Rev. D **88**, 011501 (2013).
  - [37] L. Maiani, F. Piccinini, A. D. Polosa and V. Riquer, Phys. Rev. D **71**, 014028 (2005).
  - [38] R. D'E. Matheus, S. Narison, M. Nielsen and J. M. Richard, Phys. Rev. D **75**, 014005 (2007).
  - [39] L. Maiani, A. D. Polosa and V. Riquer, Phys. Rev. Lett. **99**, 182003 (2007).
  - [40] J. Vijande, E. Weissman, N. Barnea and A. Valcarce, Phys. Rev. D **76**, 094022 (2007).
  - [41] S. Dubnicka, A. Z. Dubnickova, M. A. Ivanov and J. G. Korner, Phys. Rev. D **81**, 114007 (2010).
  - [42] Yu. S. Kalashnikova, Phys. Rev. D **72**, 034010 (2005).
  - [43] M. Suzuki, Phys. Rev. D **72**, 114013 (2005).
  - [44] T. Barnes and E. S. Swanson, Phys. Rev. C **77**, 055206 (2008).
  - [45] O. Zhang, C. Meng and H. Q. Zheng, Phys. Lett. B **680**, 453 (2009).
  - [46] R. D'E. Matheus, F. S. Navarra, M. Nielsen and C. M. Zanetti, Phys. Rev. D **80**, 056002 (2009).
  - [47] Yu. S. Kalashnikova and A. V. Nefediev, Phys. Rev. D **80**, 074004 (2009).
  - [48] P. G. Ortega, J. Segovia, D. R. Entem and F. Fernandez, Phys. Rev. D **81**, 054023 (2010).
  - [49] I. V. Danilkin and Y. .A. Simonov, Phys. Rev. Lett. **105**, 102002 (2010).
  - [50] S. Coito, G. Rupp and E. van Beveren, Eur. Phys. J. C **71**, 1762 (2011).
  - [51] S. Coito, G. Rupp and E. van Beveren, Eur. Phys. J. C **73**, 2351 (2013).
  - [52] J. Ferretti, G. Galatà and E. Santopinto, Phys. Rev. C **88**, no. 1, 015207 (2013).
  - [53] W. Chen, H. -y. Jin, R. T. Kleiv, T. G. Steele, M. Wang and Q. Xu, Phys. Rev. D **88**, no. 4, 045027 (2013).
  - [54] M. Takizawa and S. Takeuchi, PTEP **2013**, no. 9, 0903D01 (2013).
  - [55] E. Braaten and M. Kusunoki, Phys. Rev. D **69**, 114012 (2004).
  - [56] E. J. Eichten, K. Lane and C. Quigg, Phys. Rev. D **69**, 094019 (2004).
  - [57] E. Braaten, M. Kusunoki and S. Nussinov, Phys. Rev. Lett. **93**, 162001 (2004).
  - [58] E. Braaten and M. Kusunoki, Phys. Rev. D **72**, 054022 (2005).
  - [59] E. Braaten and M. Kusunoki, Phys. Rev. D **72**, 014012 (2005).
  - [60] E. Braaten, Phys. Rev. D **73**, 011501 (2006).
  - [61] C. Bignamini, B. Grinstein, F. Piccinini, A. D. Polosa and C. Sabelli, Phys. Rev. Lett. **103**, 162001 (2009).
  - [62] P. Artoisenet and E. Braaten, Phys. Rev. D **81**, 114018 (2010).
  - [63] C. M. Zanetti, M. Nielsen and R. D. Matheus, Phys. Lett. B **702**, 359 (2011).
  - [64] B. Aubert *et al.* [BaBar Collaboration], Phys. Rev. Lett. **102**, 132001 (2009).
  - [65] V. Bhardwaj *et al.* [Belle Collaboration], Phys. Rev. Lett. **107**, 091803 (2011).
  - [66] R. Aaij *et al.* [LHCb Collaboration], arXiv:1404.0275 [hep-ex].
  - [67] Y. -b. Dong, A. Faessler, T. Gutsche and V. E. Lyubovitskij, Phys. Rev. D **77**, 094013 (2008).
  - [68] F. De Fazio, Phys. Rev. D **79**, 054015 (2009) [Erratum-ibid. D **83**, 099901 (2011)].
  - [69] M. Nielsen and C. M. Zanetti, Phys. Rev. D **82**, 116002 (2010).
  - [70] T. -H. Wang and G. -L. Wang, Phys. Lett. B **697**, 233 (2011).
  - [71] T. Mehen and R. Springer, Phys. Rev. D **83**, 094009 (2011).
  - [72] S. Dubnicka, A. Z. Dubnickova, M. A. Ivanov, J. G. Koerner, P. Santorelli and G. G. Saidullaeva, Phys. Rev. D **84**, 014006 (2011).
  - [73] A. M. Badalian, V. D. Orlovsky, Y. .A. Simonov and B. L. G. Bakker, Phys. Rev. D **85**, 114002 (2012).
  - [74] M. Takizawa, S. Takeuchi and K. Shimizu, Few Body Syst. **55**, 779 (2014).
  - [75] K. Terasaki, Prog. Theor. Phys. **122**, 1285 (2010).
  - [76] D. Gamermann and E. Oset, Phys. Rev. D **80**, 014003 (2009).
  - [77] N. Li and S. -L. Zhu, Phys. Rev. D **86**, 074022 (2012).
  - [78] S. Takeuchi, M. Takizawa and K. Shimizu, Few Body Syst. **55**, 773 (2014).
  - [79] N. Brambilla, S. Eidelman, B. K. Heltsley, R. Vogt, G. T. Bodwin, E. Eichten, A. D. Frawley, A. B. Meyer *et al.*, Eur. Phys. J. C **71**, 1534 (2011).
  - [80] E. S. Swanson, Phys. Rept. **429**, 243 (2006).
  - [81] S. Godfrey and S. L. Olsen, Ann. Rev. Nucl. Part. Sci. **58**, 51 (2008).
  - [82] S. Godfrey and N. Isgur, Phys. Rev. D **32**, 189 (1985).
  - [83] S. Takeuchi and K. Shimizu, Phys. Rev. C **79**, 045204 (2009).

- 
- [84] M. Ablikim *et al.* [BESIII Collaboration], Phys. Rev. Lett. **110**, 252001 (2013).  
[85] Z. Q. Liu *et al.* [Belle Collaboration], Phys. Rev. Lett. **110**, 252002 (2013).  
[86] D. -Y. Chen, X. Liu and T. Matsuki, Phys. Rev. D **88**, no. 3, 036008 (2013).  
[87] A. Bondar *et al.* [Belle Collaboration], Phys. Rev. Lett. **108**, 122001 (2012).  
[88] P. Krokovny *et al.* [Belle Collaboration], Phys. Rev. D **88**, no. 5, 052016 (2013).  
[89] R. G. Newton, *Scattering Theory of Waves and Particles*, 2nd ed. (Springer-Verlag, New York, 1982), Chap. 17.  
[90] T. Aaltonen *et al.* (CDF Collaboration), Phys. Rev. Lett., **103**, 152001 (2009).  
[91] S. Anderson *et al.* [CLEO Collaboration], Phys. Rev. **D61**, 112002 (2000).  
[92] M. Gell-Mann, D. Sharp and W. G. Wagner, Phys. Rev. Lett. **8**, 261 (1962).  
[93] M. N. Achasov *et al.*, Phys. Rev. D **68**, 052006 (2003).  
[94] R. R. Akhmetshin *et al.* [CMD-2 Collaboration], Phys. Lett. B **578**, 285 (2004).